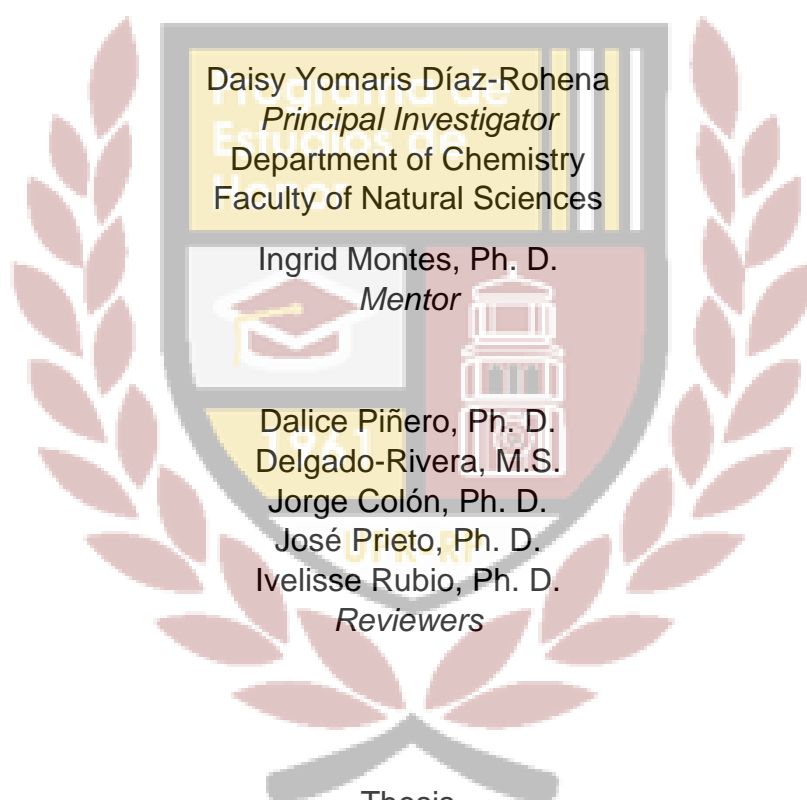


**EFFECT OF COUNTERIONS ON THE BIOLOGICAL ACTIVITY OF FERROCENYL
CHALCONE SALT DERIVATIVES: ANTIOXIDANT ACTIVITY**



Thesis
in compliance
with the requisites of
El Programa de Estudios de Honor
University of Puerto Rico
Río Piedras Campus

May 2019

University of Puerto Rico
Río Piedras Campus
Faculty of Natural Sciences
Chemistry Department



LIST OF FIGURES

LIST OF SCHEMES

LIST OF TABLES

ABSTRACT	1
1. INTRODUCTION	3
1.1. <u>Justification</u>	4
1.2. <u>Problem</u>	5
1.3. <u>Purpose</u>	6
1.4. <u>Specific aims</u>	6
1.5. <u>Research question</u>	6
1.6. <u>Limitations</u>	6
2. REVISED LITERATURE	7
2.1. <u>Ferrocene and its derivatives</u>	7
2.2. <u>Importance of pharmaceutical salts</u>	8
2.3. <u>Effect of counterions on pharmaceutical salts</u>	9
2.4. <u>Antibacterial mechanism of pyridinium salts and cationic ferrocenyl chalcones</u>	12
2.5. <u>Anion exchange chromatography</u>	12
2.6. <u>Determination of counterions</u>	15
3. METHODOLOGY	



	Pages
3.1. <u>Variables</u>	15
3.2. <u>Hypothesis</u>	16
3.3. <u>Reagents</u>	16
3.4. <u>Design</u>	17
3.4.1. <u>Preparation of salts</u>	18
3.4.2. <u>Characterization of products</u>	21
3.4.3. <u>General solubility test</u>	22
3.4.4. <u>Biological assays</u>	23
3.4.4.1. <u>Antibacterial bioassays</u>	23
3.4.4.2. <u>Anticancer and cytotoxicity bioassays</u>	23
3.4.4.3. <u>Radical scavenging activity test</u>	24
3.5. <u>Analysis of results</u>	
4. RESULTS, DISCUSSION AND FUTURE WORKS	26
4.1. <u>Characterization by NMR</u>	26
4.2. <u>Characterization by XRD crystallography</u>	36
4.3. <u>Characterization by EDS</u>	41
4.4. <u>General solubility test</u>	46
4.5. <u>Radical scavenging activity</u>	47
5. CONCLUDING REMARKS	59
ACKNOWLEDGEMENTS	59
BIBLIOGRAPHY	60
APPENDIX A: Data from literature	66

LIST OF FIGURES

Figure 1.1. Chemical structure of **1**-ferrocenyl-3-(4-N-methylpyridinium) prop-2-en-1-one and **3**-ferrocenyl-1-(4-N-methylpyridinium) prop-2-en-1-one.

Figure 1.1.1. Chemical structure of ferroquine and chloroquine.

Figure 1.1.2. Chemical structure of hydrotamoxifen and ferrocifen.

Figure 2.1. Chemical structure of ferrocene.

Figure 3.1. Method for AER (OH⁻ form) loading and ion exchange of PFC salts.

Figure 4.1. NMR peak assignments for **System 1** and **3** [PFC⁺].

Figure 4.2. **System 1** PFC salts ¹H-NMR spectra, obtained from Bruker in MeOD or D₂O, and counterion peak assignments.

Figure 4.3. **System 1** PFC salts ¹³C-NMR spectra, obtained from Bruker in MeOD or D₂O, and counterion peaks assignments.

Figure 4.4. **System 3** PFC salts ¹H-NMR spectra, obtained from Bruker in MeOD or D₂O, and counterion peaks assignments.

Figure 4.5. **System 3** PFC salts ¹³C-NMR spectra, obtained from Bruker in MeOD or D₂O, and counterion peaks assignments.

Figure 4.6. ¹H-NMR spectra of **System 3** TMB PFC salt, showing impurities.

Figure 4.2.1. Crystal structure of **System 1** chloride PFCS (R_{int} of 8.7%).

Figure 4.2.2. Crystal structure of **System 3** tosylate PFCS (R_{int} of 3.1%).

Figure 4.2.3. Crystalline unit cell of **System 3** tosylate PFCS, packing along A.

Figure 4.3.1. EDS spectra of **System 1** PFCS with various counterions.

Figure 4.3.2. EDS spectra of **System 3** PFCS with various counterions.

Figure 4.3.3. EDS spectra of attempted **System 3** fluoride m-PFCS, showing traces of Na (0.09%) and other elements.

Figure 4.3.4. EDS spectra of attempted **System 3** TMB PFCS, showing traces of I (1.06%).

Figure 4.4.1. Solubility test for **System 1** PFCS with acetate, benzoate, bromide, chloride, iodide, MeSO₄ and salicylate.

Figure 4.4.1. Solubility test for **System 3** PFCS with acetate, benzoate, bromide, chloride, iodide, MeSO₄ and salicylate.

Figure 4.4.3. Comparison of radical Scavenging Activity of PFCS from **System 1** and **System 3**, with different counterion.

Figure 4.4.4. Hardness of halides versus **System 3** PFCS antioxidant activity.

Figure 4.4.5. Hardness of halides versus **System 1** PFCS antioxidant activity.

Figure 4.4.6. Frontier density surfaces of aromatic counterions, obtained using WebMO.

Figure 4.4.7. Hardness of aromatic counterions versus **System 3** antioxidant activity.

Figure 4.4.8. Hardness of aromatic counterions versus **System 1** antioxidant activity.

Figure 4.4.9. Water solubility of sodium salts relationship to the DPPH free radical scavenging activity of **System 1** PFCS.

Figure 4.4.4. Water solubility of sodium salts versus DPPH radical scavenging activity of **System 3** PFC salts.

Figure 4.4.5. Effect of counterion mass on the DPPH free radical scavenging activity of **System 3** PFCS.



LIST OF TABLES

Table 2.1. Relationships between the properties of bioactive salts and their counterions

Table 2.2. Effect of various organic counterions on the properties of pharmaceutical salts

Table 2.3. Examples of methods used for counterion exchange in salts

Table 3.1. Preparation of PFC salts with various counterions, by applying anion exchange chromatography

Table 4.1. PFC salts with various counterions, prepared by ion exchange chromatography

Table 4.2. Signal displacements of **System 1** PFCS, as shown on $^1\text{H-NMR}$ spectra

Table 4.3. Signal displacements of **System 1** PFCS, as shown on $^{13}\text{C-NMR}$ spectra

Table 4.4. Signal displacements of **System 3** PFCS, as shown on $^1\text{H-NMR}$ spectra

Table 4.5. Signal displacements of **System 3** PFCS, as shown on $^{13}\text{C-NMR}$ spectra

Table 4.2.2. Crystal data and structure refinement of System 3 tosylate PFCS

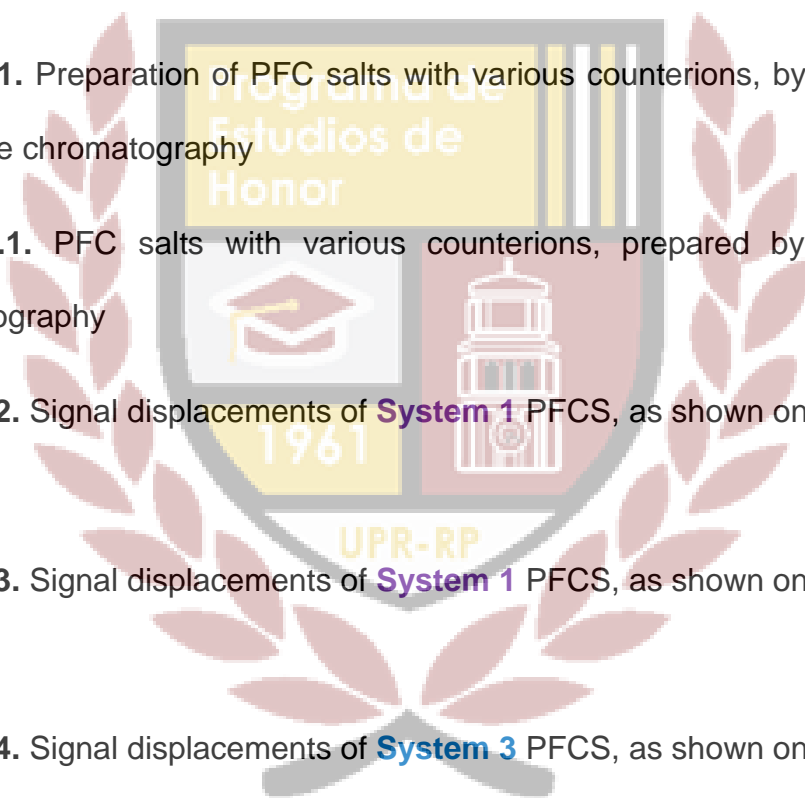


Table 4.4.1. EC₅₀ values for the antioxidant activity of System 1 and System 3 PFCS with various counterions



ABSTRACT

Over 50% of pharmaceutical compounds are administered in their salt form. Due to this high tendency, it is important to optimize the screening of novel salts to obtain the desired physicochemical properties and biological activity. Trends in the selection of counterions show that an increasing variety of anions is being considered in FDA approved drugs, apart from chloride. Counterions have shown to affect the biological activity of pharmaceutical salts, but no reliable method has been developed for the selection of the optimal counterion for bioactive salts. This sets an important limitation to the preliminary testing of the biological activity of novel compounds. Without this tool, possible drug candidates could be removed from the development pipeline due to an inappropriate pairing. In our laboratory, we are focused on the synthesis and biological properties of novel ferrocenyl chalcone derivatives. Pyridinium ferrocenyl chalcone salts paired with alkyl sulfate have been reported, showing high solubility in aqueous media. Preliminary studies showed that some salts have higher antibacterial activity when paired with iodide, compared to methylsulfate. In this research project, a wider variety of counterions are being considered to evaluate their effect on the radical scavenging and anticancer activity of these ferrocenyl chalcone salt derivatives. These include halides and the organic counterions acetate, benzoate, malate, tosylate and salicylate. To prepare these salts, previously synthesized methylsulfate or iodide salts have been subjected to ion exchange chromatography. The exchanges have been confirmed by ^1H and ^{13}C -NMR, EDS and, in some cases, via X-Ray diffraction crystallography. The bio assay results of these salts with the different anions show different values for their radical scavenging capacity. Structure-activity relationships have been hypothesized based on

the Hard and Soft Acids and Bases theory. Future works include the evaluation of the antibacterial and anticancer activity of the salts. The results of this project could lead to the selection of the optimal counterion of the ferrocenyl chalcone salt derivatives under study. These salts, due to their high solubility in water, could allow an easy method of administration, for the treatment of diseases in low-income settings.



1. INTRODUCTION

Cancer and bacterial infections rank among the deadliest health problems that threaten society. In the search for novel medicinal solutions, ferrocenyl chalcones derivatives (*Figure 1.1. System 1 and System 3*) have been an important framework for organic synthesis, as they have shown a wide range of biological applications: anticancer, antibacterial, antioxidant, antiplasmodial, among others. However, their low solubility in water has limited their application. Our laboratory previously reported the synthesis of methyl pyridinium ferrocenyl chalcone salt derivatives (P-FCS) (*Figure 1.1.*), with alkyl sulfate as their counterion.^{1,2} In contrast to most ferrocene derivatives, these salts showed high solubility in water, an important property of most orally administered drugs. Some exhibited good potential as antioxidants, and others inhibited the growth of cervical and hormone-independent breast cancer.² Their biological activity was improved or reduced, compared to their neutral parental compounds.² Preliminary work showed that, by changing the counterion of salt **3**, from methyl sulfate to iodide, the antibacterial activity of the salt is significantly enhanced.² This study aims to evaluate the effect that different counterions exert on the biological activity of these salts, in terms of their antioxidant and anticancer potential.



Figure 1.1. Chemical structure of **1**-ferrocenyl-3-(4-N-methylpyridinium) prop-2-en-1-one and **3**-ferrocenyl-1-(4-N-methylpyridinium) prop-2-en-1-one.

1.1. Justification

Chemotherapy, *Chloroquine* (Figure 1.1.1.) and antibiotics are being used to treat cancer, malaria and bacterial infections, respectively. However, they commonly accompany side-effects or lead to resistant pathogens, which complicate the medical outcomes. There is a need to develop novel and efficient alternative therapies for these diseases which together account for millions of annual deaths. In Puerto Rico, 159,030 new cases of cancer were diagnosed from 2005 to 2015, and breast cancer had the highest incidence in women. 506,508 deaths resulting from cancer were reported in that term.³ Also, the most recent report from the American Cancer Society emphasizes the need for more equitable treatment strategies, to reduce the racial gap in cancer mortality.⁴ Apart from the cancer burden, 92% of worldwide cases of malaria targeted Africa in 2017 and led to 93% of all deaths associated to this cause.⁵

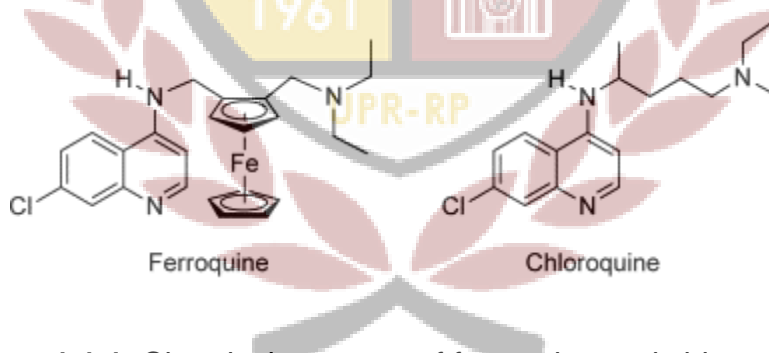


Figure 1.1.1. Chemical structure of ferroquine and chloroquine.

Ferroquine (Figure 1.1.1.), analog of chloroquine, has been found to be active even against resistant strains of *Plasmodium falciparum*, the most dangerous malaria species.⁶ This ferrocene containing drug and the anticancer drug *Ferrocifen*, analog to *Hydrotamoxifen*, continue to advance in clinical trials, showing better activity than the commercially available drugs (Figure 1.1.2). This study assesses the need to develop

strategies to specifically guide the enhancement of the drug-like properties of ferrocene derivatives. Contrary to most of FC derivatives, the PFCS that will be studied comply with the high water solubility property that is found in most orally administered drugs. They are knowingly the first of their kind to be reported.¹ No research has been found which focuses on the effect that counterions exert on the biological activity of these or related organometallic salts. Results from other studies based on structure-activity relationships support that this study could provide crucial information to decipher the mechanism of action of the novel P-FCS derivatives, which has not been confirmed.⁷

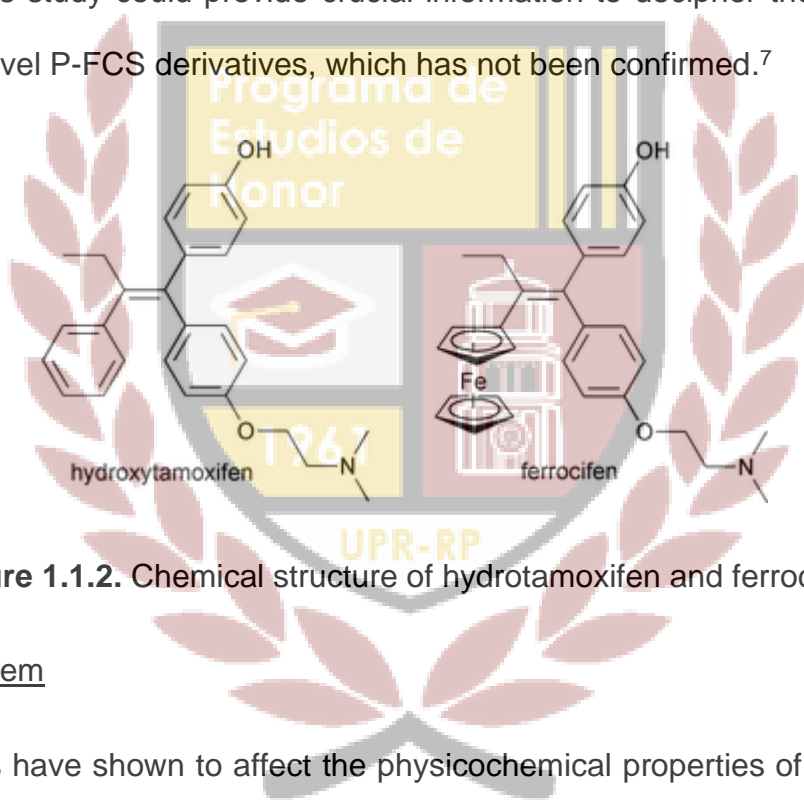


Figure 1.1.2. Chemical structure of hydroxytamoxifen and ferrocifen.

1.2. Problem

Counterions have shown to affect the physicochemical properties of salts in various ways. No reliable method has been developed to guide their selection, and a wide variety of anions has been used in drugs approved by the Food and Drug Administration (FDA).⁸ Therefore, the possibility remains, that, if the counterion plays a determining role in the mechanism of action of a treatment, potential candidates could be eliminated early in the drug development pipeline due to the inappropriate pairing of a novel salt.⁸ P-FCS derivatives have been previously synthesized, with alkyl sulfate as their counterion, and

bear promising properties with medicinal applications.² It is known that the penetration of pyridinium salts through membranes of microorganisms is influenced by the presence of a positive charge.⁹ Contrary to this, quaternization of the nitrogen atom at the 4-pyridinyl ring of **System 1** FC reduced the antibacterial property of the compounds.² As it has been studied that counterions affect the biological activity of pyridinium salts to some extent, preliminary work was done to compare the antibacterial results of PFCS with methyl sulfate and iodide counterions.^{10,2} **System 1** PFCS did not show inhibition of bacteria growth, but iodide **System 3** PFC salt showed better activity than the neutral parental chalcone.² Unknowing the effect of counterions on the aforementioned salts limits the design of their most effective form to target cancer and to suppress free radicals.

1.3. Purpose of the study

The purpose of this study is to understand the effect that different counterions have on the properties of P-FCS derivatives, previously synthesized.^{1,2} The study attempts to identify correlations between the chemical properties of the counterions and the anticancer and radical scavenging potential of P-FCS.

1.4. Specific aims

1. Prepare salts of P-FCS derivatives paired with halides and selected organic counterions
2. Characterize the products by ¹H and ¹³C Nuclear Magnetic Resonance (NMR) spectra, Electron Diffraction Spectrometry (EDS), and X-Ray Diffraction (XRD) crystallography
3. Evaluate the effect of counterions on the anticancer and radical scavenging activity of P-FCS

1.5. Research question

What effect do counterions exert on the biological activity of P-FCS derivatives?

1.6. Limitations

In this study, only *p*-methyl PFCS were considered. Other related PFCS, such as butyl pyridinium salts, will be considered in future works. The counterions evaluated on this study was limited to selected halides, carboxylates and sulfonates. However, innumerable salt forms could be possible. It was not the aim of this study to evaluate them all, but rather to evaluate representative salt forms, paired with FDA approved counterions that are commonly used. Other counterions will be explored in future works, to better support the identified structure-activity trends. The selected cancer cell lines that will be considered to test the biological activity of PFCS could be extended, to assess the principal target of these salts.

2. REVISED LITERATURE

2.1. Ferrocene and its derivatives

Ferrocene (*Figure 2.1.*) is an organometallic compound that contains two cyclopentadienyl rings in a sandwiched arrangement, coordinating a central iron atom.

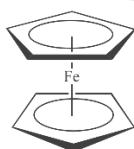


Figure 2.1. Chemical structure of ferrocene.

Ferrocene exists with Fe in the oxidation state of 2+ or, in the case of ferrocenium ions, 3+. Ferrocene and its derivatives participate in metal-specific modes of action and have

shown significant biological activity against cancer, bacteria, fungus and parasites.⁶ Another drug-like property of ferrocene is its low toxicity.¹ *Ferroquine*, analogous to *Chloroquine*, is currently in phase-2 clinical trials, showing a promising potential against malaria, which ranks among the deadliest infectious diseases.¹¹ In preclinical evaluations, *Ferrocifen* has shown more activity against hormone dependent breast cancer than the commercial *Tamoxifen*.¹² These promising drug candidates have motivated the incorporation of ferrocenyl groups in organic synthesis, in the search for novel effective drugs. Among ferrocenyl derivatives, ferrocenyl chalcones have been synthesized through Claisen Schmidt reactions. This scaffold has been used to insert a variety of functional groups, obtaining promising *in-vitro* results regarding their biological activity. Different strategies have been employed to overcome their low aqueous solubility, which presents a limitation for their clinical use as orally administered drugs. Recently, our laboratory reported the synthesis of novel P-FC derivatives, and the resulting pH independent salts, achieved through N-alkylation. ¹H and ¹³C-NMR spectra of these alkyl sulfate salts were obtained for characterization purposes.¹

2.2. Importance of Pharmaceutical Salts

Salts can increase the aqueous solubility and dissociation rate of pharmaceutical formulations. These properties are related to a higher compatibility of the drugs with the aqueous media found inside of the human body, and their enhanced absorption, due to a more efficient transportation across membranes.¹³ Other techniques for increasing aqueous solubility exist, such as complexation with cyclodextrins, but salt formation is among the few that conserve the molecule of the active pharmaceutical ingredient or induce minimal changes to it.⁸ Additionally, salts typically are the most stable form of a

drug and undergo crystallization. This facilitates further processing steps, like purification and isolation, and provides longer shelf lives.¹³ Hence, salts are commonly employed during the preparation of effective drugs.

2.3. Effect of counterions on pharmaceutical salts

The early stages for selecting an optimal salt must consider the counterion, since it can influence the physicochemical properties of the product, in terms of: solubility, dissolution rate, hygroscopicity, stability, impurity profiles, and crystal characteristics.⁸ Also, it can affect the biological activity and bioavailability of pharmaceutical salts.

The common-ion effect is known to reduce the bioavailability of chloride salts.¹⁴ Due to this effect, although chloride is most commonly found among the salts approved by the FDA, trends are shifting towards a wider range in the selection of anions, many of them being considered as safe, such as salicylate.^{8,13} For making predictions regarding likely candidates, it is necessary to understand the role of counterions on the properties of pharmaceutical salts. *Table 2.1* describes specific examples found in the literature regarding the counterion dependence of bioactive salts.

Table 2.1. Relationships between the properties of bioactive salts and their counterions

Property of the counterions	Correlation with salt properties
Solubility	The hydration potential of the counterion correlated to the overall trend of solubility of sulfonate salts of <i>Prazosin</i> . The mesylate salt,

	<p>which presented the highest solubility, also presented the highest bioavailability in rat models treated orally.¹⁴</p>
Hydrophobicity	<p>The <i>Gram-positive</i> antibacterial activity of amino acid-based hydrogelating amphiphiles was shown to improve by increasing the hydrophobicity of the carboxylate counterions. It was proposed, that this property of the anions assisted the amphiphiles during their penetration through the lipid bilayer membrane of bacteria.⁷</p> <p>Another study prepared salts parting from several carboxylic acid drugs and amines. It was found that increasing the hydrophobicity of the ammonium cations resulted in the reduction of the solubility of products.¹⁵</p>
Alkyl chain length	<p>Antibacterial tests showed that increasing the alkyl chain length of counterions moderately limited their antibacterial activity. This tendency of the counterions was related to their increasing hydrophobicity or decreasing polarity.¹⁶</p>
Steric Hinderance	<p>Bulky counterions can control the coplanarity of pyridinium salts, which can affect the biological activity of compounds, as is the case for FC derivatives.¹⁷</p>
Kosmotropic and chaotropic properties, and charge density of anions	<p>The smaller the hydrated radius of anions, the more they enhanced the destabilizing potential of pyridinium salts towards model membranes, but this was not completely consistent. It was analyzed that their activity also depends on the nature of the</p>

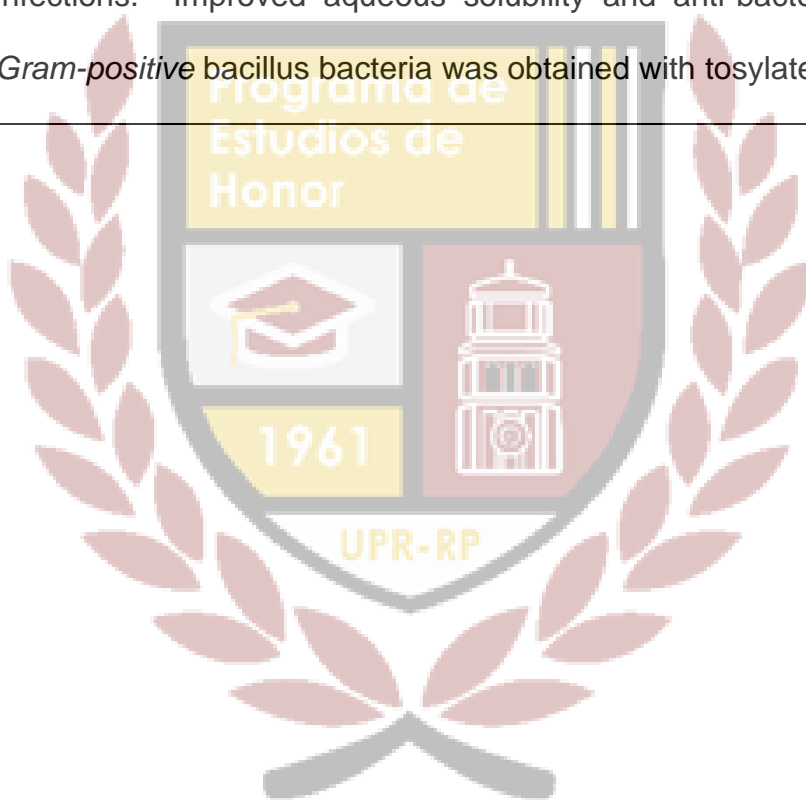
	anions, if they are kosmotropes or chaotropes, as they exert opposite effects on the solubility of solutes. ⁹
--	--

The formation of a salt is generally guided by the “rule of three”: there must be a difference of at least three pK_a units between the acid and base of the conjugate pair.¹⁸ Another consideration is that, if the free acid or base of the counterion admits high biological activity, it can allow a relatively lower dosing of the drug to achieve a clinical effect.¹⁹ Studies have attempted to eliminate non-optimal salt forms until the choice is narrowed down. Others have employed a related series of counterions, to achieve a systematic study that relates their properties with the effectivity of the drug.¹⁵ In this study, the organic counterions have been selected based on the knowledge of their previous use and effectivity in drugs (*Table 2.2.*).

Table 2.2. Effect of various organic counterions on the properties of pharmaceutical salts

Counterion	Study results
oxalate	The oxalate salt of <i>Ethionamide</i> , an anti-tuberculosis drug of poor aqueous solubility, exhibited the highest bioavailability and dissolution rate, compared to cocrystals of glutaric acid, adipic acid, suberic acid, sebacic acid and fumaric acid. ¹⁸
malate	In comparison to traditional supplements, calcium lactate salts containing malate as their counterion have shown increased solubility and bioavailability. <i>Enalapril malate</i> showed significantly lower

	hygroscopicity, higher solubility, good solid state stability and better flow, in comparison to the marketed maleate salt. ²⁰
acetate	<i>Glatiramer acetate</i> , also used for treating multiple sclerosis, demonstrated potential against <i>Gram-negative</i> bacteria. ²¹ Acetic acid presented high antibacterial activity against <i>E. coli</i> . ²²
tosylate	<i>Tinidazole</i> is a low soluble antiparasitic drug used against <i>Protozoan</i> infections. Improved aqueous solubility and anti-bacterial activity in <i>Gram-positive</i> bacillus bacteria was obtained with tosylate salts. ²³



2.4. Antibacterial mechanism of pyridinium salts and cationic chalcones

It has been previously studied that both quaternary pyridinium salts and cationic chalcone antibiotics with aliphatic amino substituents have a mechanism of action that involves the disruption of bacterial cell membranes.^{9,10} This is consistent with the fact that those membranes possess negatively charged phospholipids. This allows for the establishment of strong electrostatic interactions between the chalcone and the surface of bacteria.¹³ While the lipophilic interaction between the chalcone and the interior of the membrane is retained, this leads to a potent compound with reduced affinity and toxicity towards eukaryotic cells, which bear neutral zwitterionic phospholipids on their membranes.¹³

2.5. Anion Exchange Chromatography

Anion exchange is achieved through chromatography. The medium comprises of spherical particles, substituted with cationic groups, bound with exchangeable counterions. This technique is frequently employed, because it requires only four simple steps: equilibration, sample application and wash, elution and regeneration.²³ This selective separation technique is dependent on the net surface charge of the ions or compounds, and of the medium. Some general criteria can be considered in the prediction of the affinity order of the counterions in the resin, based on: (1) the solvated size of the solute ion, (2) the degree of cross-linking of the ion exchange resin, (3) the polarizability of the solute ion, (4) the ion exchange capacity of the ion exchanger, (5) the functional group on the ion exchanger and (6) the degree to which the solute ion interacts with the ion exchange matrix.²⁵

A current challenge is to achieve the exchange between monovalent and divalent anions, which is restricted by the high charge affinity of anion exchange resins (AERs). Glycidol has been used to manipulate the selectivity of anion exchange resins towards divalent species.²⁵ Subsequent derivatizations with glycidol was reported to significantly reduce the retention of divalent species on the resin, resulting in their elution before bromide and nitrate.²⁶ Various methodologies for achieving ion exchange in salts are presented in *Table 2.3*.



Table 2.3. Examples of methods used for counterion exchange in salts

Summary of the method	Description
Anion exchange chromatography: halide-to-anion exchange	<p>Anion loading: Load AERs (OH⁻ form) with the desired counterion (A⁻) by treating it with the corresponding aqueous acid solution or ammonium salt.²⁷</p> <p>Anion exchange: Swap halides of a salt to A⁻ by passing a solution of the salt through the AER (A⁻ form) in the appropriate solvent, according to the hydrophobicity of the eluent salt.²⁷</p>
Nitrogen quaternization using dimethyl carbonate, and acid addition	Quaternate a nitrogen with dimethyl carbonate and react the obtained quaternary ammonium salt with an organic acid containing carbonate groups (Ex. acetic, propionic, butanoic, hexanoic, octanoic and decanoic). ²⁸
Nitrogen quaternization using methyl iodide and precipitation of AgI	Dissolve an iodide salt in CH ₃ OH and add an equimolar quantity of the appropriate dissolved [Ag ⁺][A ⁻] salt. Mix the solution at room temperature. After a few minutes, some white AgI precipitate begins to form. Filter the mixture after about 30–45 min, collect the liquid phase and evaporate its solvent. ²⁹

2.6. Determination of counterions

Several methods have been employed to determine the counterion of a pharmaceutical salt. Ion chromatography (IC) and Ultra-High-Performance Liquid Chromatography (UHPLC) with Charged Aerosol Detection (CAD) and/or UV detection are most commonly used. If crystalline samples are available, X-ray diffraction crystallography is the preferred tool for characterization, and it can be combined with Infrared (IR), Raman, and Nuclear Magnetic Resonance (NMR) spectroscopies.¹³ A benefit of NMR characterization on this study is that the proton displacements of pyridinium cations vary depending on their π -electron polarization, which is affected by the nature of the counterions.^{30,31} By combining ¹H-NMR spectra with crystal structures, this electron density has been related to the coplanarity of pyridinium cations, both influenced by the anion of choice.²⁵ Similarly, the chemical shift of the carbonyl on FC derivatives has been related to the planarity of the compounds and the degree of polarization of this group, which can affect the radical scavenging potential of FC derivatives.¹⁷ Other methods of determination of counterions, although less sensitive than those mentioned above, include potentiometric titration and gravimetric analysis using the silver nitrate test or the chromate test.^{27,29} Alcalde, et al. (2012) used the chromate test for quantitation iodide content after a halide-to-anion exchange procedure. However, this research used Electron Dispersive Spectroscopy, which not only detects atoms, but also calculates their percent weight on the sample (% wt.).

3. METHODOLOGY

3.1. Variables

- Dependent variables: counterions of PFCS (halides or organic counterions); system of PFCS (System **1** or **3**); cancer cell lines and bacteria (refer to *Design*)
- Independent variables: minimal inhibitory concentration (MIC) of PFCS against bacteria proliferation, 50% effective concentration (EC₅₀) against DPPH free radicals, and cancer cell growth percent (cell growth %); chemical shifts of signals in ¹H and ¹³C-NMR spectra

3.2. Hypothesis

By varying the counterion of PFCS derivatives, their anticancer, antibacterial and radical scavenging potential is affected, and it follows a structure-activity tendency.

3.3. Reagents

1. Acetic acid used as received.
2. Amberlite® IRA-400 (Cl) ion exchange resin (Aldrich Chemical Co.) used as received.
3. Amberlite® IR-45 (OH) ion exchange resin used as received.
4. Amberlyst A-26 (OH) ion Exchange resin (Aldrich Chemical Co.) used as received.
5. Benzoic acid dissolved before use.
6. Deuterium oxide (99.9 %) (Aldrich Co.) used as received.
7. Deuterated methanol (99%) (Sigma Aldrich) used as received.
8. L-malic acid (98-100 %) (Sigma Chemical Co.) used as received.
9. Hydrochloric acid (36.9%) (Fisher Scientific) diluted before use.
10. Methanol (99.9 %) (Fisher Chemical) used as received.

11. Methyl sulfate pyridinium ferrocenyl chalcone salt, previously synthesized by Sara M. Delgado-Rivera, previously dissolved before use.
12. Salicylic acid (99 %) (Sigma-Aldrich Co.) dissolved before use.
13. Sodium chloride (99.0 %) (BDH) dissolved before use.
14. Sodium fluoride (99 %) (Sigma-Aldrich Co.) dissolved before use.
15. (L)-potassium tartrate monobasic (K-TMB) (Sigma-Aldrich Co.) dissolved before use.
16. Tetrabutylammonium bromide (TBA-Br) (≥ 98.0 %) (Sigma-Aldrich Co.) dissolved before use.
17. p-toluene sulfonic acid monohydrate, ACS reagent (98.5%) (Sigma-Aldrich Co.) dissolved before use.

3.4. Design

This study requires quantitative methods and its design is experimental. This methodology includes the general procedures that will be followed, and references to the corresponding protocols. The P-FCS that will be used are **System 1** P-FCS and **System 3** PFCS (*Figure 1.1*).

3.4.1. Preparation of salts

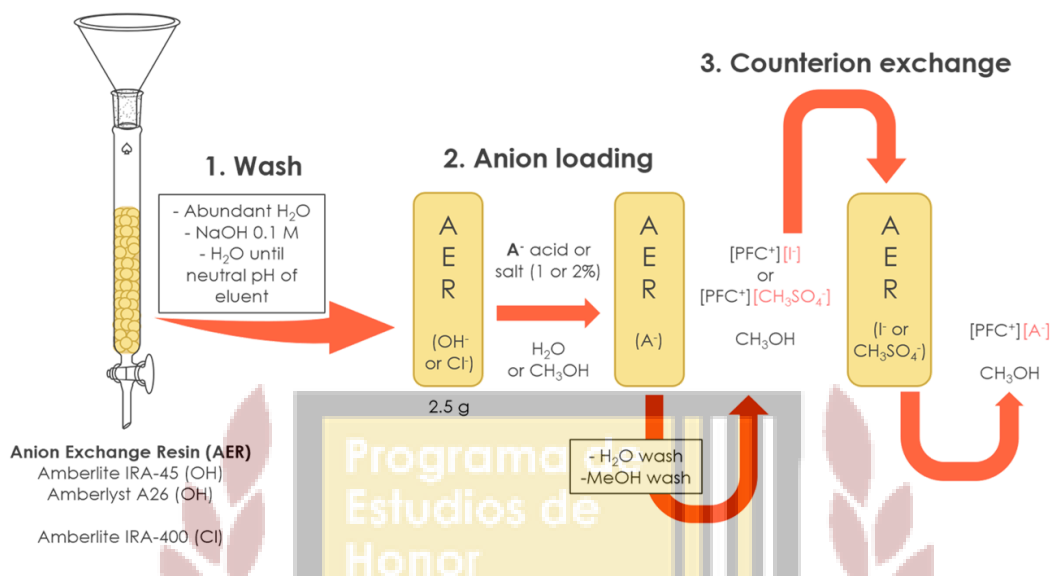


Figure 3.1. Method for AER (OH⁻ form) loading and ion exchange of PFC salts.²⁷ For AER (Cl⁻ form), NaOH was replaced with 0.1 M HCl wash.

Anion exchange chromatography has been applied to exchange the counterion of PFC salts to the followings: acetate, benzoate, bromide, chloride fluoride, iodide, tosylate, salicylate and tartrate monobasic. These counterions have been selected due to their known use in previously approved in FDA formulations, and because they are therefore generally considered as safe.⁸

The halide-to-anion exchange methodology, previously developed by Alcalde, et al. (2012) was followed for a variety of counterion exchanges including anion-to-halide and halide-to-halide exchanges (*Table 3.1*).

Table 3.1. Preparation of PFC salts with various counterions, by applying anion exchange chromatography

Counterion	Starting salt (System and counterion)	Amberlite AER	Anion loading solution
Acetate	1 or 3-[PFC ⁺][I ⁻]	IRA-45 (OH)	2% Acetic acid (aq)
Benzoate	3-[PFC ⁺][I ⁻]	IRA-45 (OH)	1% benzoic acid (aq)
Bromide	1 or 3-[PFC ⁺][MeSO ₄ ⁻]	A26 (OH)	1% TBABr (aq)
Chloride	1-[PFC ⁺][MeSO ₄ ⁻] or 3-[PFC ⁺][I ⁻]	IRA-400 (Cl)	0.1 M HCl (aq)
Fluoride	3-[<i>m</i> PFC ⁺][I ⁻]	IRA-400 (Cl)	Saturated NaF (aq)
Malate	1 [PFC ⁺][I ⁻]	A26 (OH)	1% Malic Acid (aq)
Salicylate	1 or 3-[PFC ⁺][I ⁻]	A26 (OH)	2% Salicylic acid (MeOH)
Tosylate	1 or 3-[PFC ⁺][I ⁻]	A26 (OH)	1% PTSA (aq)
Tartrate (TMB)	3-[PFC ⁺][I ⁻]	A26 (OH)	Saturated TMBK (aq)

Anion exchange resins, originally in their hydroxide (OH⁻) form, were mixed in distilled water and packed into a micro column. A washing step was done to ensure purity of the resins. This consisted in adding an abundant volume of distilled water (> 75 mL), followed by a wash of NaOH 0.1 M (25 mL). A wash of distilled water was done until obtaining a neutral pH in the eluent, to ensure the removal of excess OH⁻ ions. 1% or 2% w/v aqueous solutions of the acids of the

desired counterions were added to the columns. In some cases, considering the solubility of the acids, MeOH was used instead as a solvent for these solutions, and considering the high reactivity of the acids, a salt of the desired counterion was used instead for anion loading (*Table 3.1*).

For tracking the loading of counterions to the resin, the pH or halide content of the eluents was determined. The acids (or salt solutions) were added until the pH of the eluent changed from basic to acidic (or neutral, if salts were used), tracked with Litmus paper. This confirmed that OH^- had been displaced from the resin and that an excess of the acid (or salt) had been added. For the TBA-Br salt solutions, anion loading was tracked using the Silver Test instead. A positive silver test on the eluent confirmed that the resin was saturated with bromide. Resins were washed with distilled water until neutral pH or removal of excess halides (confirmed by obtaining a negative result on the Silver Test of the eluent), followed by MeOH to displace water.

Ensuring that the columns were efficiently packed, 28-45 mg of I^- PFC salts, previously dissolved in 10 mL of MeOH, were added to the columns. An additional MeOH wash was done to ensure the complete elution of the product. The eluent was collected and MeOH was evaporated under pressure. During this methodology and storage, the PFC salts were protected from light exposure by covering all flasks and equipment with foil.

For the exchanges to chloride, a similar methodology was followed. Anion exchange resin, originally in Cl^- form were used instead, and the NaOH wash was

replaced by 0.1 M HCl (aq) wash, which also served the purpose of loading the resin with the desired counterion, Cl⁻. Silver halide test

The eluent from the resins was added to an assay tube, containing a diluted solution of HNO₃ and 3 drops of AgNO₃. Formation of a precipitate confirmed presence of bromide or chloride on the eluent, and therefore, that the resin was overloaded with those halides. If no precipitate formed, this confirmed the absence of those halides on the eluent.

3.4.2. Characterization of the products:

The products were dissolved in deuterated methanol (CD₃OD) or deuterated oxide (D₂O) and their ¹H and ¹³C-NMR spectra were obtained using a Bruker (Dx 300, 500 or 700) system. CD₃OD signals were calibrated to δ 3.31 ppm in ¹H-NMR spectra and to δ 49.00 ppm in ¹³C-NMR spectra. These spectra were compared to the reported ones for the parental PFCS (iodide or methyl sulfate form) and further analyzed to confirm the presence of the desired counterions.¹ If products readily crystallized after evaporation of MeOH under pressure, X-Ray crystallography structures were obtained in collaboration with Dr. Dalice Piñero at the XRD facility at UPR Molecular Research Center. ED spectra were obtained from EDS-EDAX Genesis 2000, at the Materials Characterization facilities from UPR Molecular Research Center, to confirm the absence or presence of halides and sulfur.

3.4.3. General solubility test:

The solubility of the PFCS with different counterions was tested in water. 1.0 mL of distilled water was added to 1.0 mL of PFCS, or the equivalent (*Table 3.2*). Solubility was reported based on observation: “high” if PFCS dissolved immediately, “moderate” if they dissolved partially, and “low” if they barely dissolved. Products with “moderate” and “low” solubility were sonicated, but the solubility barely improved.

Table 3.2. Mass of PFCS and volume of distilled water used for the general solubility test

Counterion	System 1	System 3 mg
	m PFCS / V H ₂ O	m PFCS / V H ₂ O
acetate	12 mg / 1.2 mL	11 mg / 1.1 mL
benzoate	11 mg / 1.0 mL	11 mg / 1.1 mL
bromide	10 mg / 1.0 mL	11 mg / 1.1 mL
chloride	10 mg / 1.0 mL	10 mg / 1.0 mL
iodide	11 mg / 1.1 mL	10 mg / 1.0 mL
MeSO ₄	11 mg / 1.1 mL	6 mg / 0.6 mL
salicylate	10 mg / 1.0 mL	11 mg / 1.1 mL
tosylate	10 mg / 1.0 mL	11 mg / 1.1 mL

3.4.4. Biological Assays

The products have been tested for free radical scavenging activity and will be tested for activity against cancer and bacteria growth. The same protocol used by Delgado-Rivera (2017) will be followed, to be able to compare the bioactivity results with those previously obtained for other closely related PFC salts.²

3.4.4.1. Antibacterial bioassays

The protocol used by Delgado-Rivera (2017) and Sanabria et al. (2014) will be followed to test the products in triplicate against the following bacteria: *Staphylococcus aureus* and *Escherichia coli*.^{2,32} The stock cultures will be kept in blood agar. Subcultures will be incubated for maximum of 1 day at 37 °C on TSA. Suspension cultures will be prepared by inoculation of single colonies in Trypticase Soy Broth (TSB). Susceptibility testing will be carried out by adding the P-FCS products in DMSO and TSB to wells that contain colonies. MIC will be determined to be the concentration at which P-FCS prevent turbidity in the well after maximum 1-day incubation.

3.4.4.2. Anticancer and cytotoxicity bioassays

The protocol reported by Vaskova, J. and Perjesi, P. (2015) and Delgado-Rivera, S. (2017) will be followed to test the products in triplicate against the following cell lines: estrogen independent breast cancer (MDA-MB-231), cervical cancer (HeLa), prostate cancer (PC-3); and lung fibroblast cells (MCR-5).^{2, 33} The cells will be cultured in growth medium, and tested for viability and counted using trypan blue stain. Cells will be seeded into 96-well plates and a 25 µM solution of

the P-FCS product will be added, dissolved in dimethyl sulfoxide (DMSO). 3-(4,5-dimethylthiazol-2-yl)-5-(3-carboxymethoxyphenol)-2-(4-sulfophenyl)-2H-tetrazolium (MTS) colorimetric solution will be added after a period of incubation. The absorbance of the cells at 490 nm will be measured against the positive control cell line, and cell growth % will be calculated.

3.4.4.3. Radical scavenging activity test

The products were tested against DPPH free radicals, as described by Sharma, O., Bhat, T. (2008) and Delgado-Rivera, S. (2017).^{2,34} Ascorbic acid was used as standard, DPPH as the positive control, and P-FCS solutions as the tested compounds and background interference. 12 methanolic solutions of each P-FCS product or ascorbic acid was prepared, in the range from 300 to 0.1 μ M, by serial dilution. 96-well plates were prepared with triplicates of experimental, control and standard wells. 50 μ L of the previously mentioned PFCS solutions were added to the experimental wells, and, for the standard wells, ascorbic acid solutions. 50 μ L of 0.1 M DPPH methanolic solution was added to the experimental and standard wells. 50 μ L of MeOH was added to the negative control wells. For the positive control wells, 50 μ L of 0.1 M DPPH methanolic solution and 50 μ L of methanol were plated.

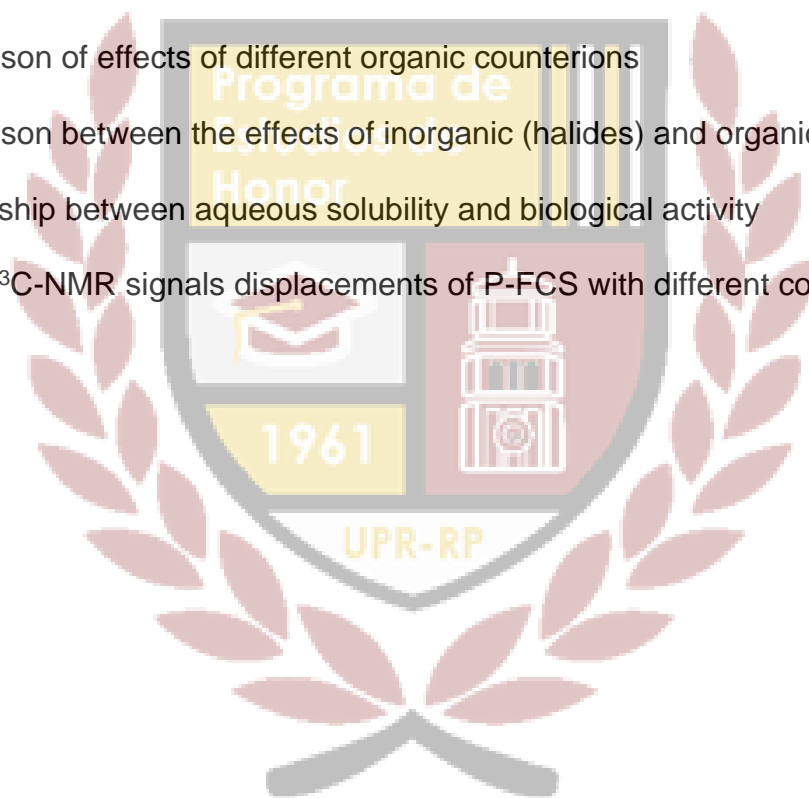
Using a Plate Reader (Thermo Scientific™ Multiskan™ GO UV/Vis microplate spectrophotometer), the absorbance of the plated solutions was measured at 517 nm after 15 minutes of DPPH exposition. Dose-response curves were generated using GraphPad Prism® biostatistics software to determine the

EC₅₀, the efficient concentration of the tested compound necessary to allow only 50% of the free DPPH radical concentration.

3.5. Analysis of results

The results of the radical scavenging assays have been analyzed by considering the following, and the same comparisons will be done in future works:

- Comparison of effects of different halides
- Comparison of effects of different organic counterions
- Comparison between the effects of inorganic (halides) and organic counterions
- Relationship between aqueous solubility and biological activity
- ¹H and ¹³C-NMR signals displacements of P-FCS with different counterions



4. RESULTS, DISCUSSION AND FUTURE WORKS

Table 4.1. PFC salts prepared by ion exchange chromatography, to study the effect of the counterions on their biological activity

Counterion	System 1 PFCS	System 3 PFCS
Acetate	✓	✓
Benzoate	✓	✓
Bromide	✓	✓
Chloride	✓	✓
Fluoride		
Iodide	✓	✓
Tosylate (PTS)	✓	✓
Salicylate	✓	✓
Tartrate monobasic		

✓: Product was obtained

4.1. Characterization by NMR

The ^1H -NMR (Figure 4.2. and 4.4.) and ^{13}C -NMR (Figure 4.3. and 4.5.) spectra of PFCS show characteristic signals of their corresponding counterions. Some signals do not appear (shown in gray in Figure 4.2-4.5). This has been attributed to the low resolution of some spectra, for example, due to the inability of the instrument to lock the solvent, as was the case for the NMR spectra of **System 1** salicylate PFCS. No decomposition product was detected, but for the attempted **System 3** TMB, the

obtained NMR shows significant impurities (*Figure 4.6.*). Halide salts do not show any additional signal, apart from the ones of the cation, [PFC⁺]. The displacement of signals on the ¹H and ¹³C-NMR spectra of salts of each PFCS system have been compared (*Tables 4.2-5*). The low standard deviation between the values suggest that there is no significant difference between the displacement of the signals from [PFC⁺] **System 1** or **System 3**. However, it has been identified on the ¹³C-NMR (*Figure 4.2.*) of **System 1** bromide PFCS, that this bromide salt presents an upfield displacement of the ipso carbons (**d** and **h**), connecting ferrocenyl and pyridinium to the chalcone moiety.

Figure 4.1. NMR peak assignments for **System 1** and **3** [PFC⁺].

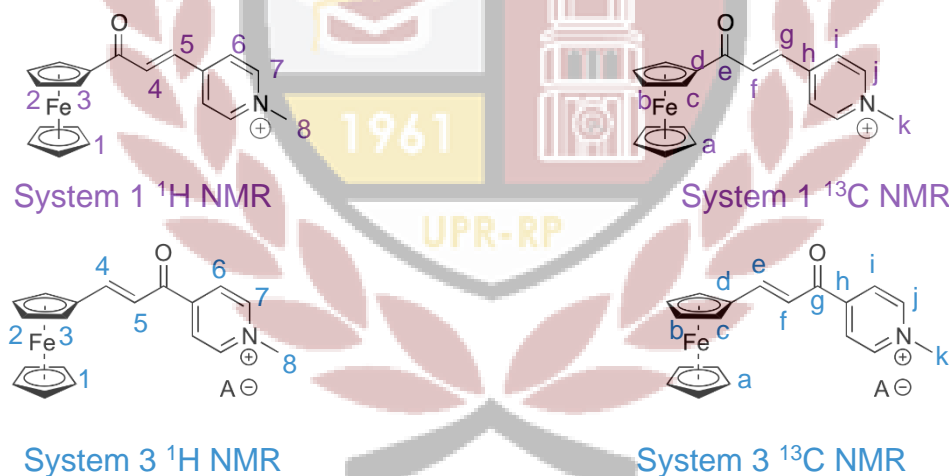


Figure 4.2. System 1 PFC salts $^1\text{H-NMR}$ spectra, obtained from Bruker in MeOD or D_2O , and counterion peak assignments

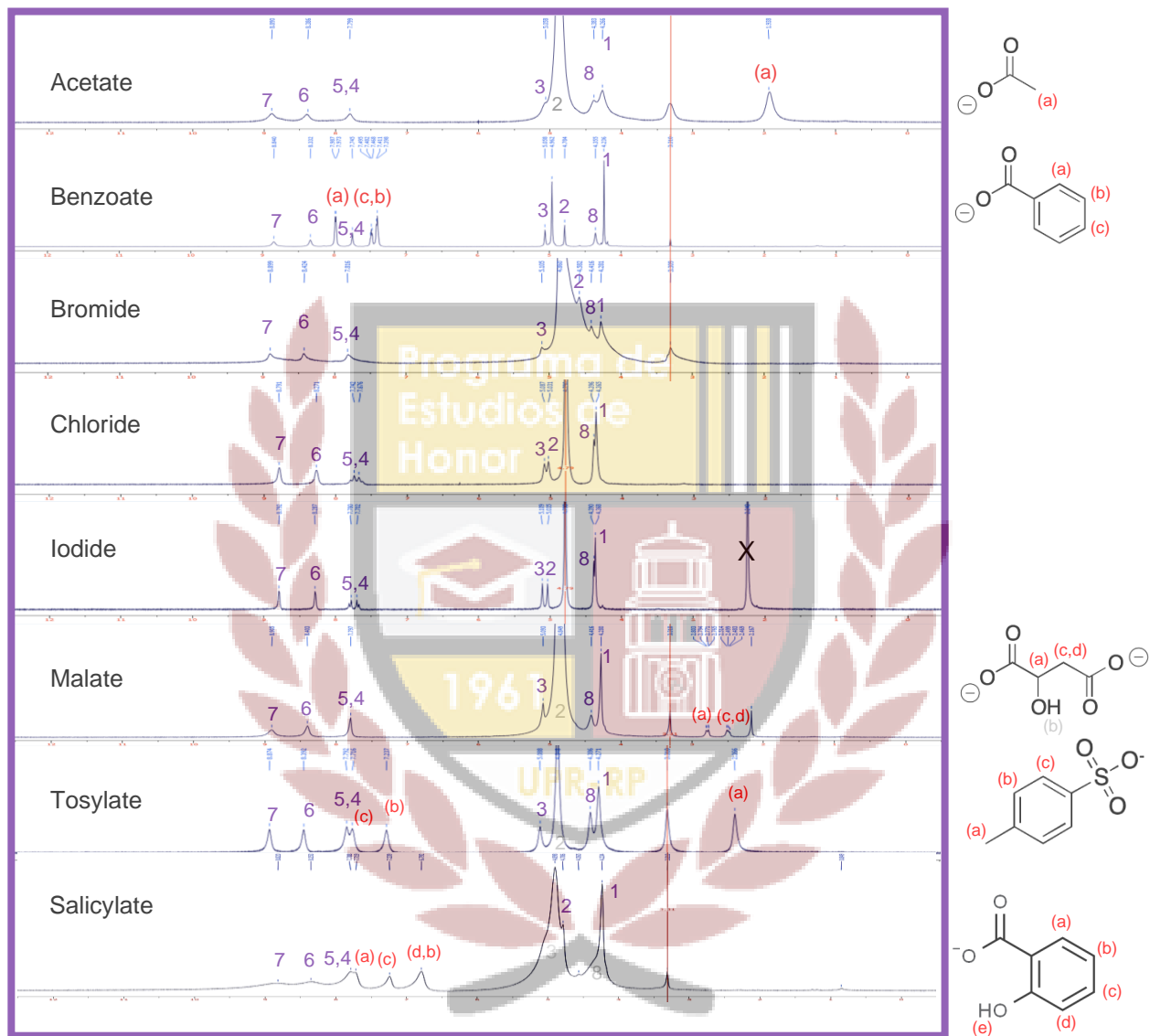


Table 4.2. Signal displacements of **System 1** PFCS, as shown on $^1\text{H-NMR}$ spectra^{a,b}

Counterion	$^1\text{H-NMR}$ Signal displacements, δ (ppm)							
	7	6	4	5	3	2	8	1
MeSO ₄ ¹	8.73	8.20	7.57	7.69	5.02	4.97	4.35	3.73
Acetate	8.89	8.39	8.8	8.8	5.06	---	4.38	4.27
Salicylate	8.82	8.35	7.78	7.78	---	4.79	---	4.23
Benzoate	8.84	8.33	7.75	7.75	5.06	4.78	4.36	4.24
Tosylate	8.87	8.39	7.79	7.79	5.01	----	4.39	4.27
Bromide	8.90	8.42	7.82	7.82	5.11	4.58	4.42	4.28
Iodide	8.79	8.29	7.70	7.78	5.11	5.04	4.39	4.37
Chloride	8.79	8.27	7.67	7.74	5.09	5.03	4.40	4.37
Standard Deviation	0.06	0.07	0.4	0.4	0.04	0.2	0.02	0.2

^a --- : Signal is not observed on $^1\text{H-NMR}$ (refer to *Figure 4.2*).

^b Counterions were ordered in terms of their antioxidant activity, to facilitate the identification of a trend.

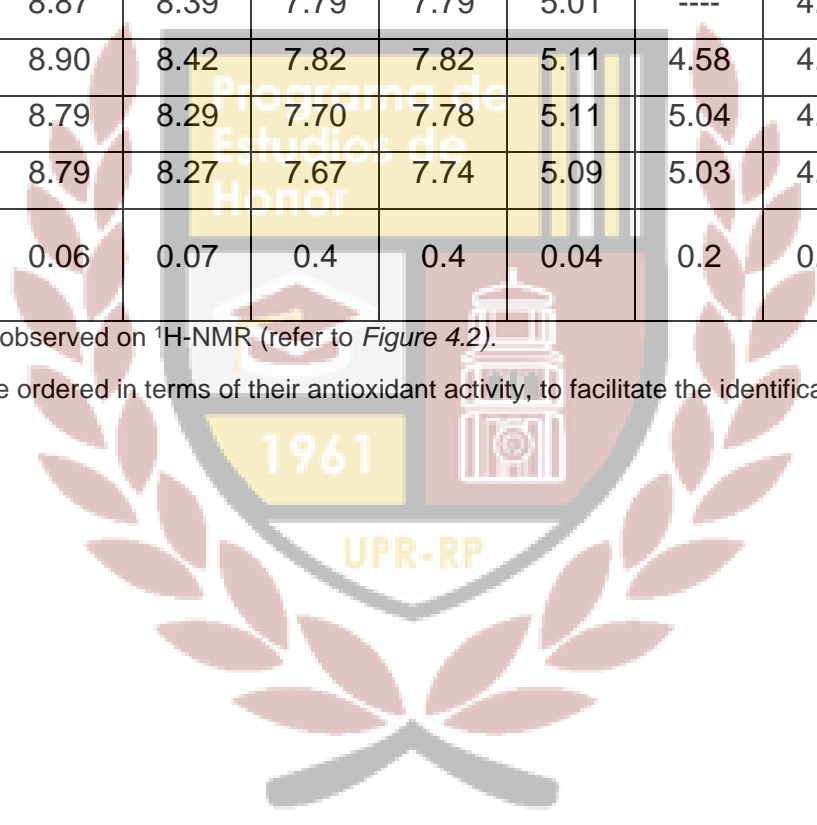


Figure 4.3. System 1 PFC salts ^{13}C -NMR spectra, obtained from Bruker in MeOD or D_2O , and counterion peaks assignments

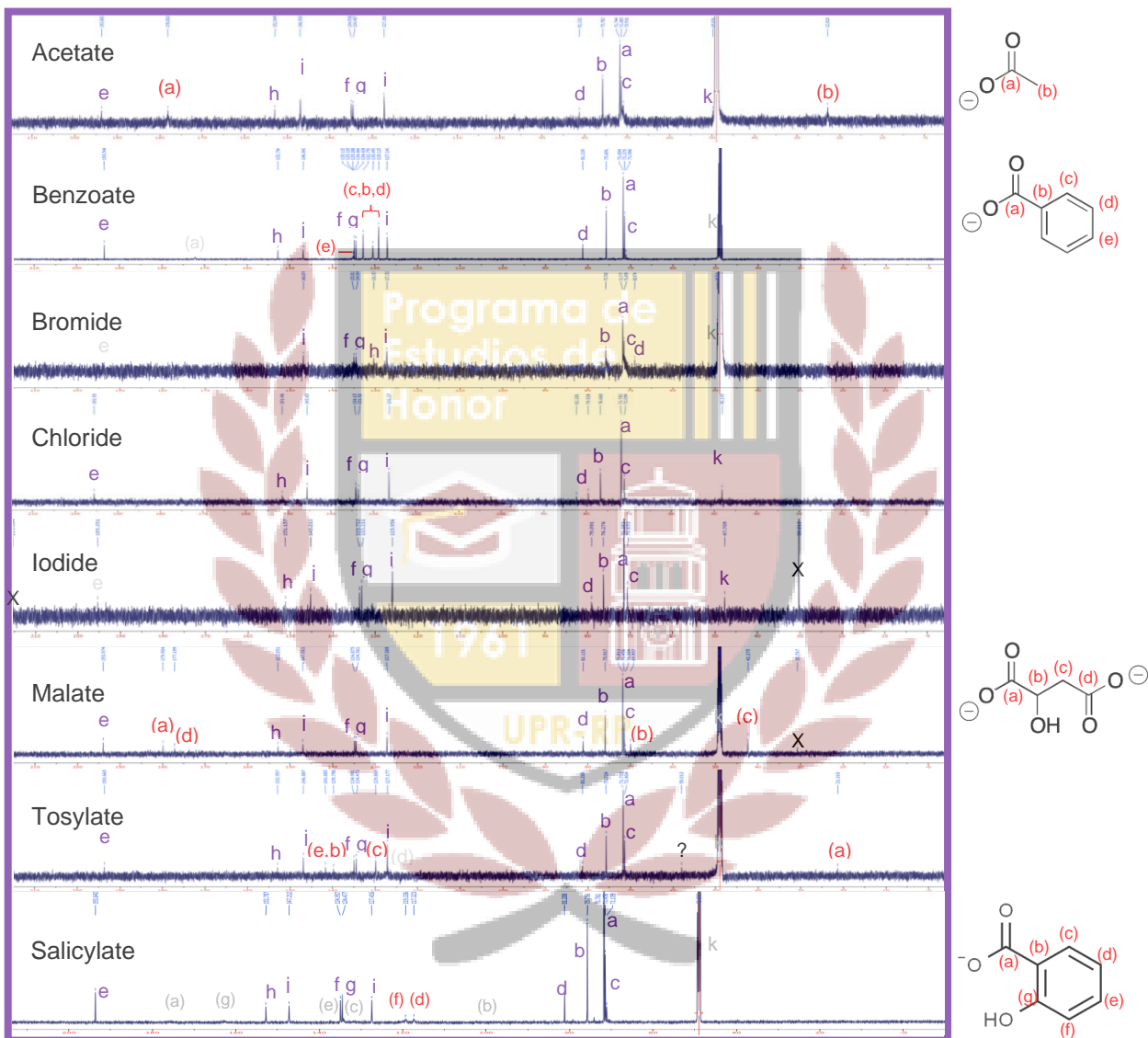


Table 4.3. Signal displacements of **System 1** PFCS, as shown on ^{13}C -NMR spectra^{a-c}

Counterion	^{13}C -NMR Signal displacements, δ (ppm)										
	e	h	j	f	g	i	d	b	a	c	k
MeSO ₄ ¹	194.4	150.5	145.0	133.6	132.6	126.8	79.0	75.9	71.1	70.4	47.5
Acetate	193.7	152.9	146.9	134.9	134.5	127.2	81.2	75.8	71.7	71.4	49.8
Salicylate	193.6	152.8	147.2	135.0	134.5	127.4	81.2	75.8	71.8	71.5	---
Benzoate	193.5	152.7	146.8	135.1	135.1	127.1	81.2	75.7	71.7	71.4	---
Tosylate	193.7	153.0	146.9	135.0	134.5	127.2	81.3	75.7	71.7	71.4	---
Bromide	---	130.4	146.9	135.0	134.4	127.3	69.0	75.8	71.8	71.5	49.5
Iodide	195.4	151.2	145.2	133.7	133.2	126	79.1	76.3	71.4	70.7	47.7
Chloride	195.6	151.5	145.6	134.2	133.5	126.4	82.3	76.7	71.8	71.1	48.1
Standard Deviation	0.9	8.0	0.9	0.6	0.8	0.5	4.0	0.4	0.2	0.4	1.0

a --- : Signal is not observed on ^{13}C -NMR (refer to *Figure 4.3*).

b Counterions were ordered in terms of their antioxidant activity, to facilitate the identification of a trend.

Figure 4.4. System 3 PFC salts $^1\text{H-NMR}$ spectra, obtained from Bruker in MeOD or D_2O , and counterion peaks assignments

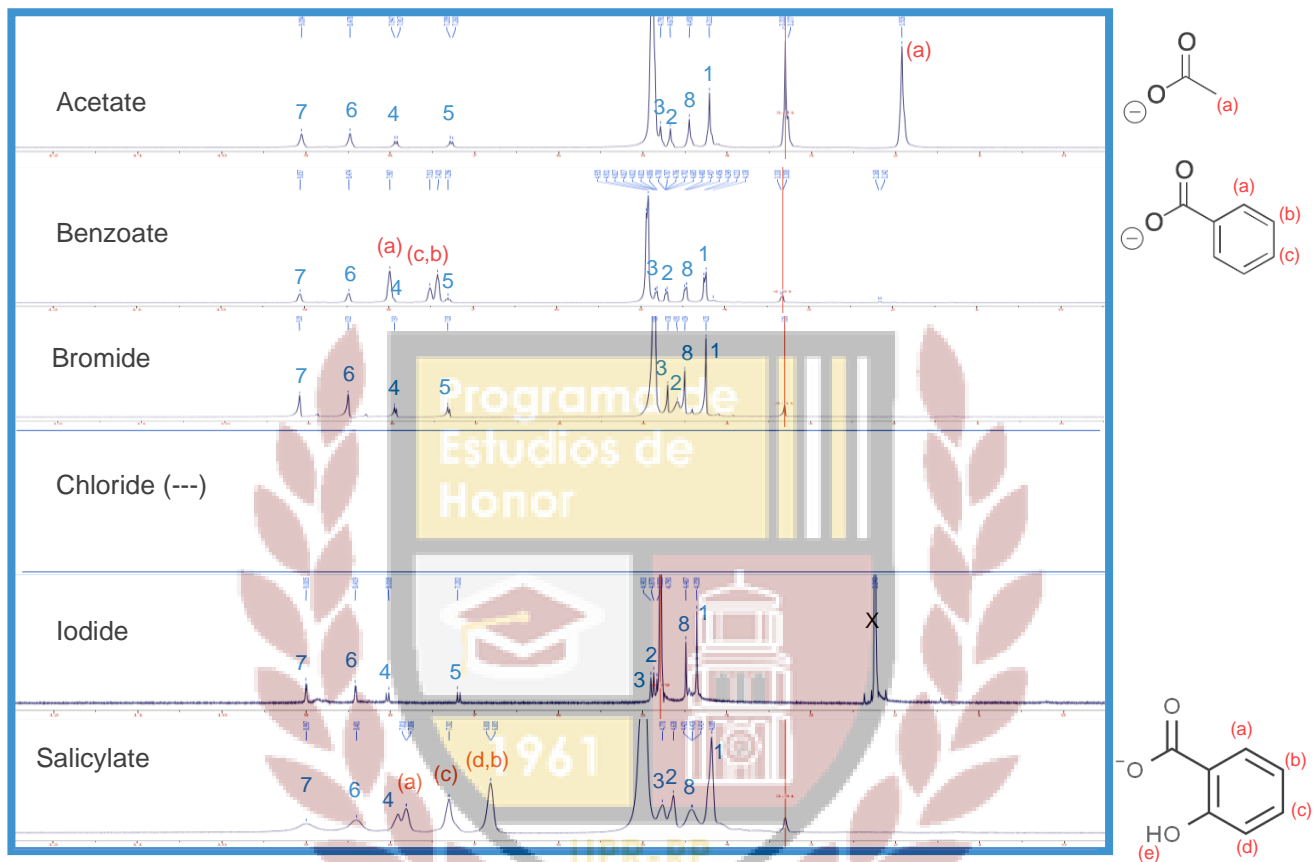


Table 4.4. Signal displacements of **System 3** PFCS, as shown on $^1\text{H-NMR}$ spectra^{a-c}

Counterion	$^1\text{H-NMR}$ Signal displacements, δ (ppm)							
	7	6	4	5	3	2	8	1
Iodide	9.01	8.42	8.02	7.20	4.9	4.87	4.49	4.36
Benzoate	9.06	8.47	---	7.30	4.82	4.64	4.46	4.24
Salicylate	9.00	8.40	---	---	4.77	4.64	4.42	4.19
MeSO_4^1	8.95	8.35	7.90	7.11	5.09	5.04	4.46	4.29
Acetate	9.05	8.48	7.93	7.51	4.79	4.68	4.45	4.21
Bromide	9.11	8.53	7.97	7.34	4.71	4.59	4.50	4.25
Chloride	---	---	---	---	---	---	---	---
Standard Deviation	0.06	0.06	0.05	0.2	0.1	0.2	0.03	0.06

^a --- : Signal is not observed on $^1\text{H-NMR}$ (refer to *Figure 4.4*) or data is not available.

^b Counterions were ordered in terms of their antioxidant activity, to facilitate the identification of a trend.

^c System 3 tosylate salt NMR spectra were not obtained, but crystal structure is available.

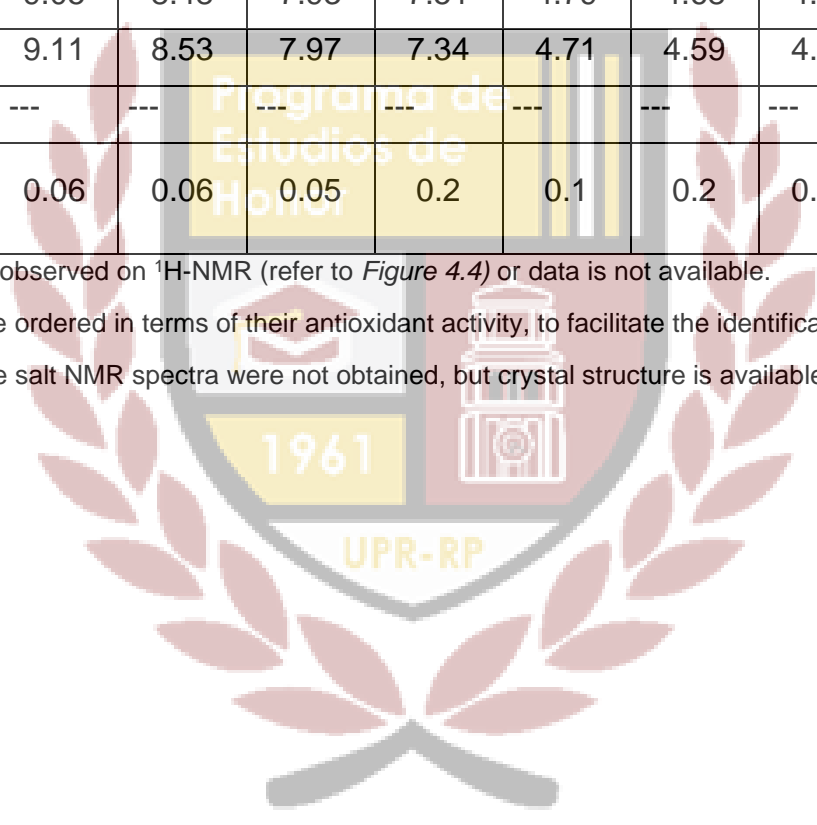


Figure 4.5. System 3 PFC salts ^{13}C -NMR spectra, obtained from Bruker in MeOD or D_2O , and counterion peaks assignments

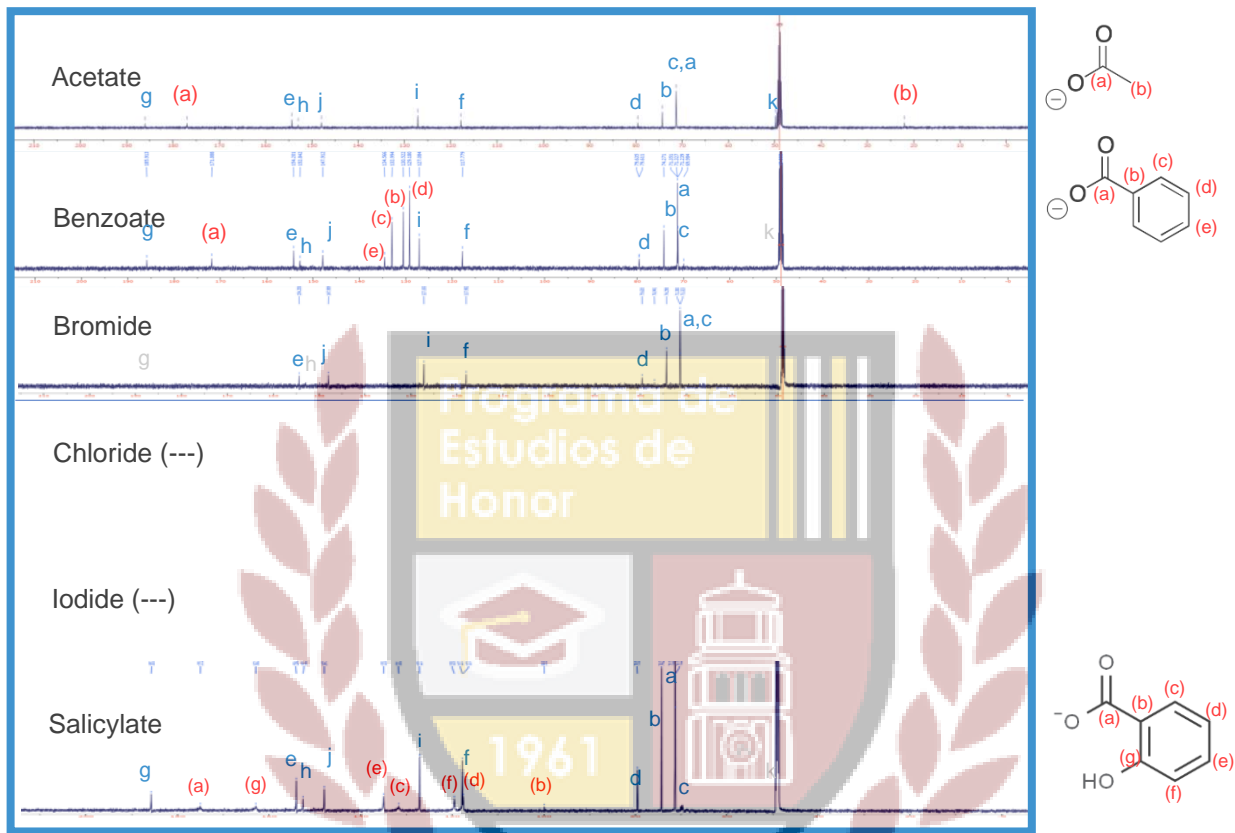


Table 4.5. Signal displacements of **System 3** PFCS, as shown on ^{13}C -NMR spectra^{a-c}

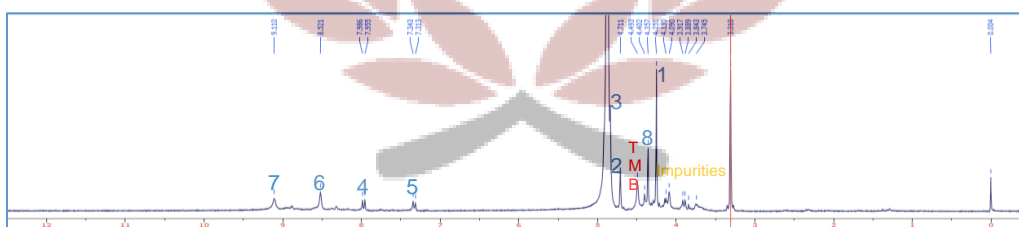
Counterion	^{13}C -NMR Signal displacements, δ (ppm)										
	g	e	h	j	i	f	d	b	a	c	k
Iodide	---	---	---	---	---	---	---	---	---	---	---
Benzoate	185.9	154.2	152.8	147.9	127.1	117.8	79.6	74.3	71.3	70.0	---
Salicylate	185.8	154.1	152.6	148.0	127.1	117.8	79.6	74.3	71.4	71.3	---
MeSO ₄ ¹	186.8	154.9	151.3	146.3	126.1	116.8	78.1	74.2	70.8	70.6	55.4
Acetate	186.1	154.3	153.0	148.0	127.1	117.8	79.6	74.3	71.3	71.3	49.9
Bromide	---	154.4	---	148.0	127.2	118.0	76.9	74.3	71.4	71.3	---
Chloride	---	---	---	---	---	---	---	---	---	---	---
Standard Deviation	0.5	0.3	0.8	0.8	0.5	0.5	1.0	0.04	0.3	0.6	4.0

^a --- : Signal is not observed on ^1H -NMR (refer to *Figure 4.5*) or data is not available.

^b Counterions were ordered in terms of their antioxidant activity, to facilitate the identification of a trend.

^c System 3 tosylate salt NMR spectra were not obtained, but crystal structure is available.

Figure 4.6. ^1H -NMR spectra of **System 3** TMB PFC salt, showing impurities



4.2. Characterization by XRD crystallography

System 1 chloride PFCS and **System 3** tosylate PFCS readily crystallized after evaporation of MeOH under pressure, forming monocrystals. Apparently, the choice of the counterion for these salts can facilitate the purification step, which gains more importance in pharmaceutical processes. Their crystalline structure of those salts was elucidated with good and excellent correlations, respectively, with an R_{int} of 8.7% (at 100 K) for **System 1** chloride salt (*Figure 4.2.1.*) and of 3.1% (at 300 K) for **System 3** tosylate salt (*Figure 4.2.2.*). Both structures show the negatively charged counterion near the positive alkylated nitrogen of $[\text{PFC}^+]$, in a 1:1 ratio, with no counterions interacting with Fe^{2+} from ferrocene. However, the unit cell of **System 3** tosylate salt (*Figure 4.2.3.*), shows a special interaction between tosylate and ferrocene, presumably a π - π interaction due to the aromatic nature of their rings.

The $[\text{PFC}^+]$ cation of both Systems, **1** and **3**, show a highly planar structure, with only the ferrocene moiety showing a tridimensional structure. This high planarity is said to confer high antioxidant activity to ferrocenyl chalcones, due to a more efficient delocalization of electrons.³⁶

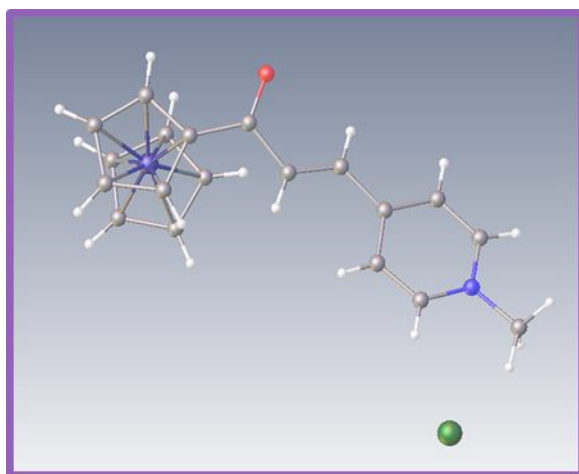


Figure 4.2.1. Crystal structure of **System 1** chloride PFCS (R_{int} of 8.7%).



Table 4.2.1. Crystal data and structure refinement of **System 1** chloride PFCS

Empirical formula	C ₁₉ H ₁₈ ClFeNO
Formula weight	367.64
Temperature/K	100
a/Å	10.32330(10)
b/Å	5.67450(10)
c/Å	30.4380(4)
α/°	90
β/°	95.0670(10)
γ/°	90
Volume/Å ³	1776.08(4)
Z	4
μ/mm ⁻¹	8.206
F(000)	760.0
Index ranges	-12 ≤ h ≤ 12, -5 ≤ k ≤ 6, -36 ≤ l ≤ 36
Reflections collected	27607
Independent reflections	3187 [R _{int} = 0.0873, R _{sigma} = 0.0415]
Goodness-of-fit on F ²	1.063

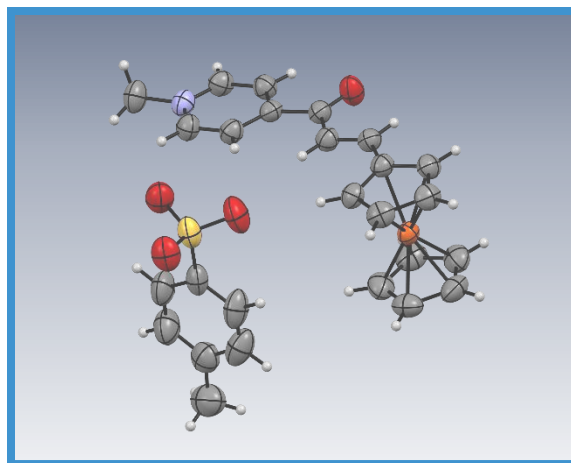


Figure 4.2.2. Crystal structure of **System 3** tosylate PFCS (R_{int} of 3.1%).

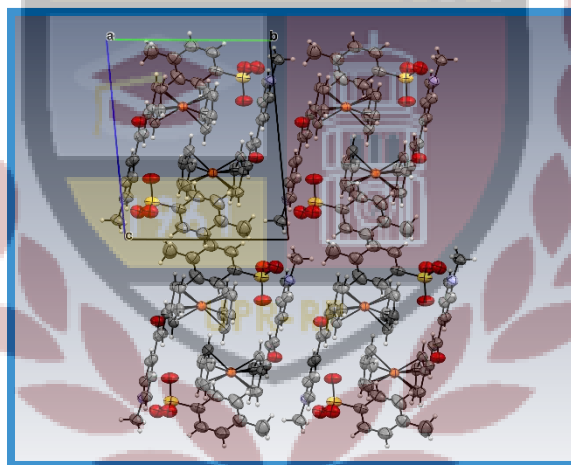


Figure 4.2.3. Crystalline unit cell of **System 3** tosylate PFCS, packing along plane A.

Table 4.2.2. Crystal data and structure refinement of System 3 tosylate PFCS

Empirical formula	C ₁₉ H ₁₈ ClFeNO
Formula weight	367.64
Temperature/K	100
a/Å	9.33308 (1)
b/Å	10.2582 (1)
c/Å	12.5890 (2)
α/°	82.682 (1)
β/°	79.843 (1)
γ/°	78.887 (1)
Volume/Å ³	1158.48 (3)
Z	2
μ/mm ⁻¹	6.338
F(000)	524.0
Radiation	CuKα (λ = 1.54184)
Reflections collected	4049
Independent reflections	[R _{int} = 0.0311]
Goodness-of-fit on F ²	1.029

4.3. Characterization by EDS

EDS results were used to confirm complete counterion exchanges, with special focus on the detection of Cl, Br, I and S atoms, due to their presence in starting materials ([PFC⁺][I⁻] or [MeSO₄]) or the desired salt forms ([PFC⁺][Cl⁻],[Br⁻] and [PTS⁻]). All counterion exchanges that were done using the halide-to-anion exchange chromatography method, starting from [PFC⁺][I⁻] (I = 20.63% wt. for **System 1** and 18.62% wt. for **System 3**), proceeded with complete exchange, showing no iodide presence on their EDS spectra (I = 0 % wt.) (*Figure 4.3.1. and 4.3.2.*). This was true even for organic counterions with higher molecular weight than iodide: salicylate and tosylate. This goes against the trend that anion exchange resins have more affinity towards counterions of higher molecular weight.²⁴ Also, this finding further extends the application of the halide-to-anion exchange method. For exchanges from MeSO₄ to Br, an anion-to-halide exchange was done which also goes against the molecular weight trend. Traces of sulfate atom were detected (≤0.48% wt.), but this is not considered significant. Other elements, some not used during the exchanges, were found in traces in some samples: Si, Al, Na and Cl. These could come from the silica chromatography resin used during the purification of the parental PFC neutral compounds, the aluminum sample holder of the EDS, Na⁺ from NaOH wash during ion exchange, and Cl⁻ from the distilled water used instead of nanopure water, respectively, or from trace impurities of the reagents used during ion exchanges. Counterion exchange to F⁻ was confirmed for **System 3 meta** PFCS (*Figure 4.3.3.*), starting from the iodide salt. However, NaF was used, and sodium salts are known to offer poor exchange yields. Since Na was detected

in trace amounts, this exchange was not further explored, limited by the only F⁻ salt available at the laboratory. In future works, this exchange can be attempted using other F⁻ salt to load this anion to the resin. The trace amounts of iodide on **System 3** TMB PFCS salt could explain the additional signals observed on the NMR (*Figure 4.3.4.*).



Figure 4.3.1. EDS spectra of **System 1** PFCS with various counterions

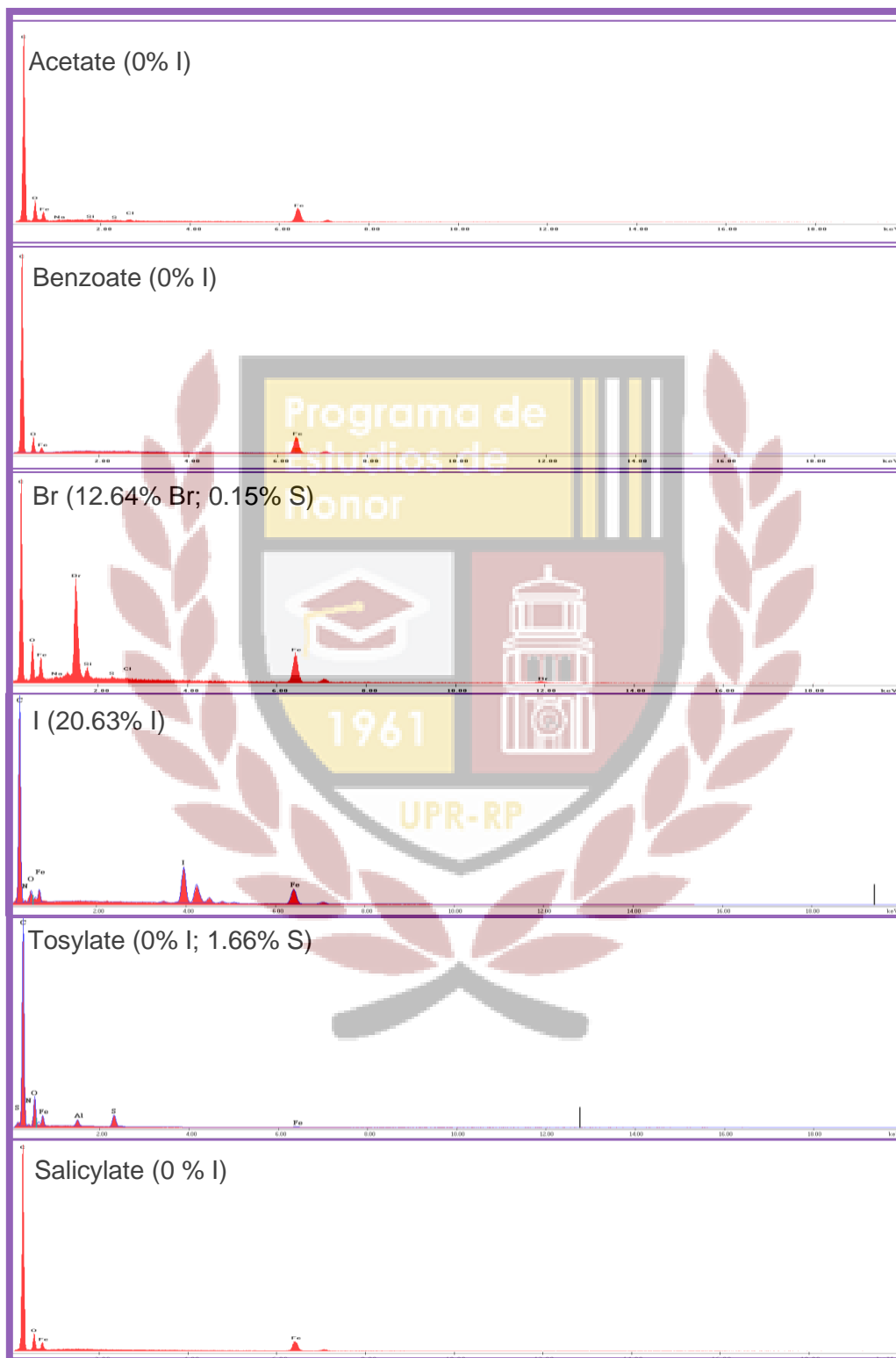


Figure 4.3.2. EDS spectra of **System 3** PFCS with various counterions

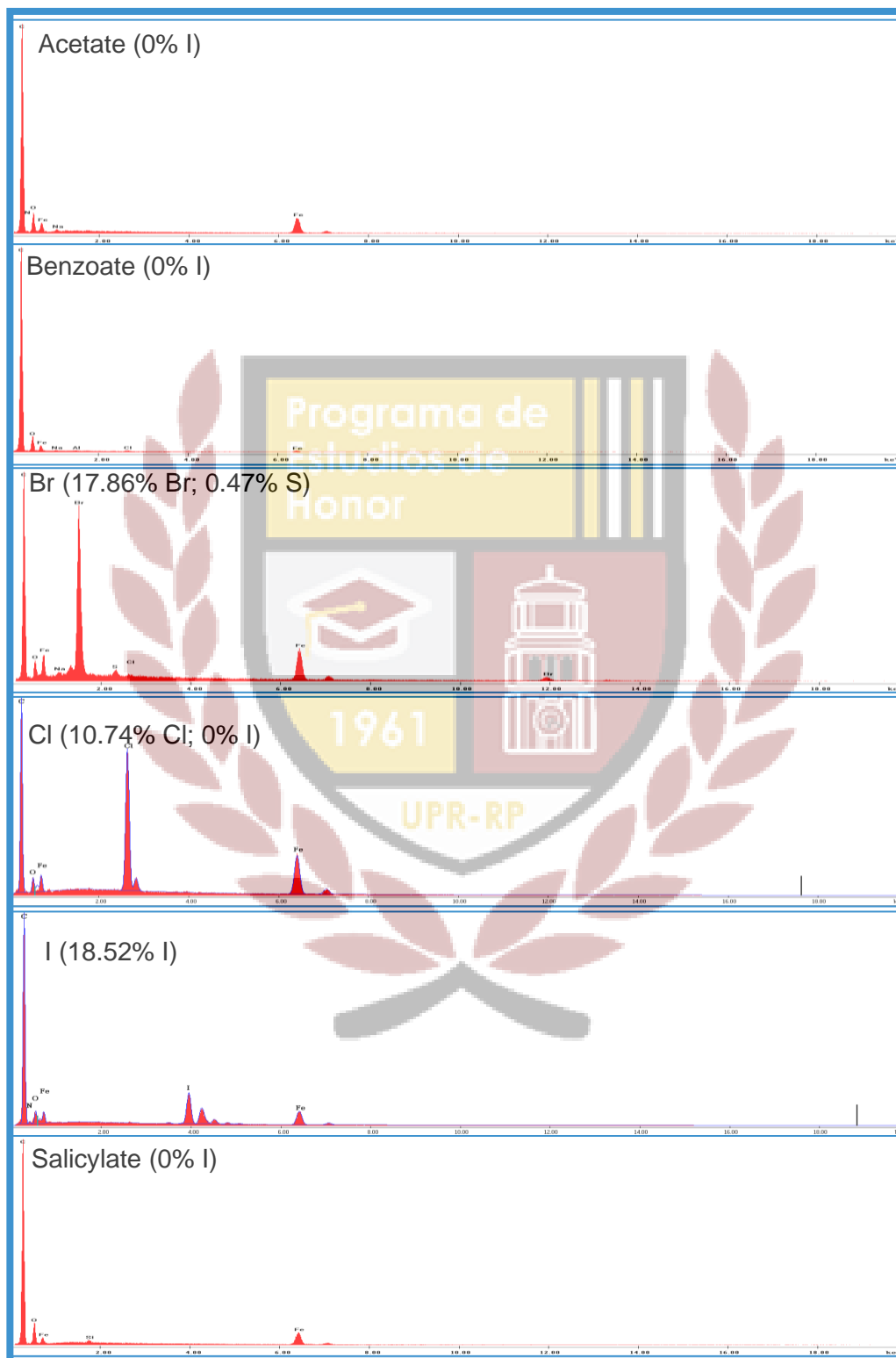


Figure 4.3.3. EDS spectra of attempted **System 3** fluoride m-PFCS, showing traces of Na (0.09%) and other elements.

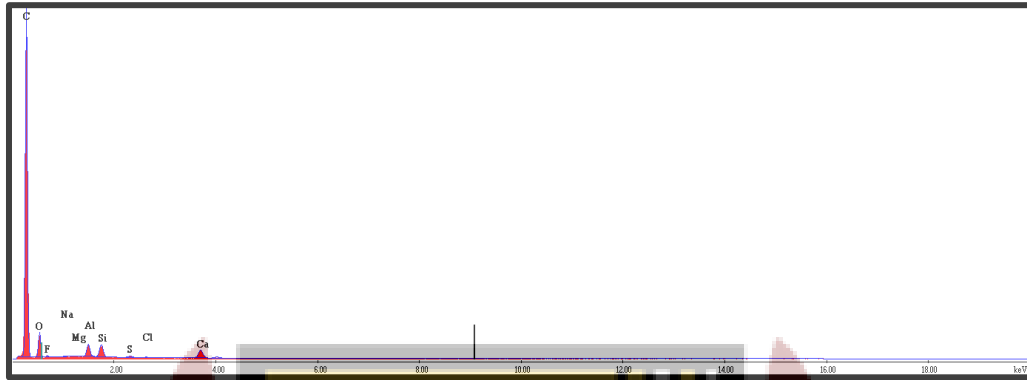
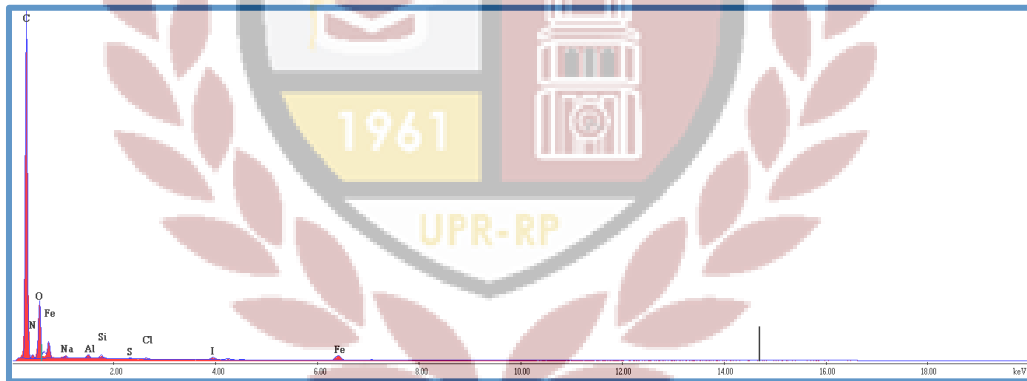


Figure 4.3.4. EDS spectra of attempted **System 3** TMB PFCS, showing traces of I (1.06%)



4.4. General solubility test

In a 1:1 (w/v) proportion of PFCS and distilled water, 10 PFCS salts were highly soluble in water, 2 showed moderate solubility and 4 had low solubility (*Table 4.4.1 and Figure 4.4.1*). Aromatic counterions provided the lowest solubility. Benzoate and salicylate, closely related carboxylates provided low solubility for both systems of PFCS. Tosylate provided moderate solubility, again, for both systems. Salts with halides, acetate and methylsulfate readily dissolved in distilled water. Since the solubility did not differ between systems, differences in solubilities have been attributed to a counterion effect. For example, benzoate and salicylate, closely related carboxylates provided low solubility for both systems PFCS. More specifically, the order of solubility for PFCS with aromatic counterions was: tosylate > benzoate > salicylate (*Figure 4.4.2*).

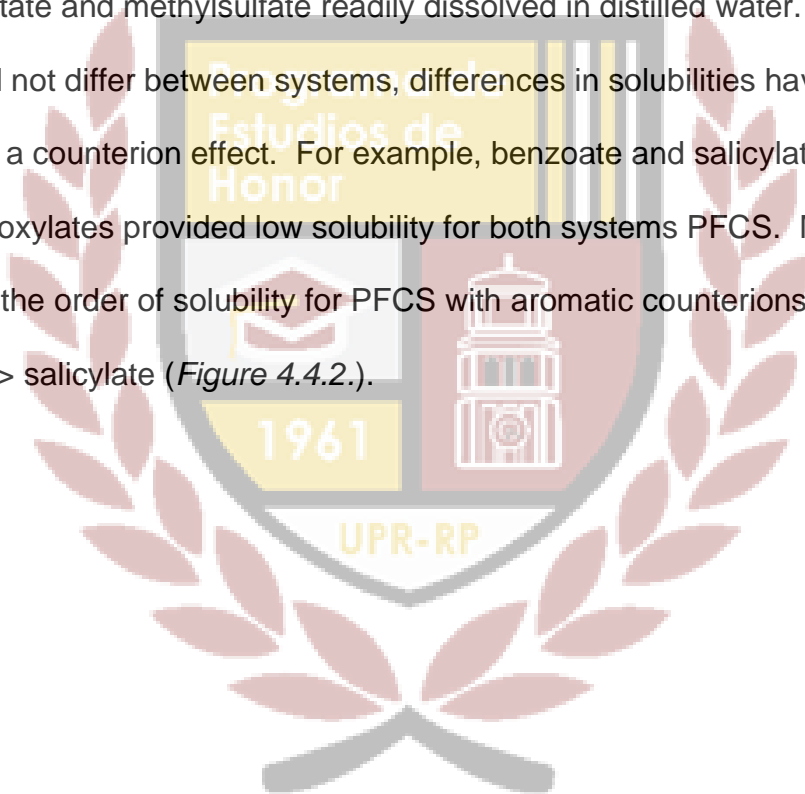


Table 4.4.1. General solubility of PFCS in water in a 1:1 (w/v) proportion

Counterion	System 1 solubility	System 3 solubility
Acetate	High	High
Benzoate	Low	Low
Bromide	High	High
Chloride	High	High
Iodide	High	High
MeSO ₄	High	High
Salicylate	Low	Low
Tosylate	Moderate	Moderate



Figure 4.4.1. Solubility test for **System 1** PFCS with acetate, benzoate, bromide, chloride, iodide, MeSO₄, **tosylate and salicylate**.

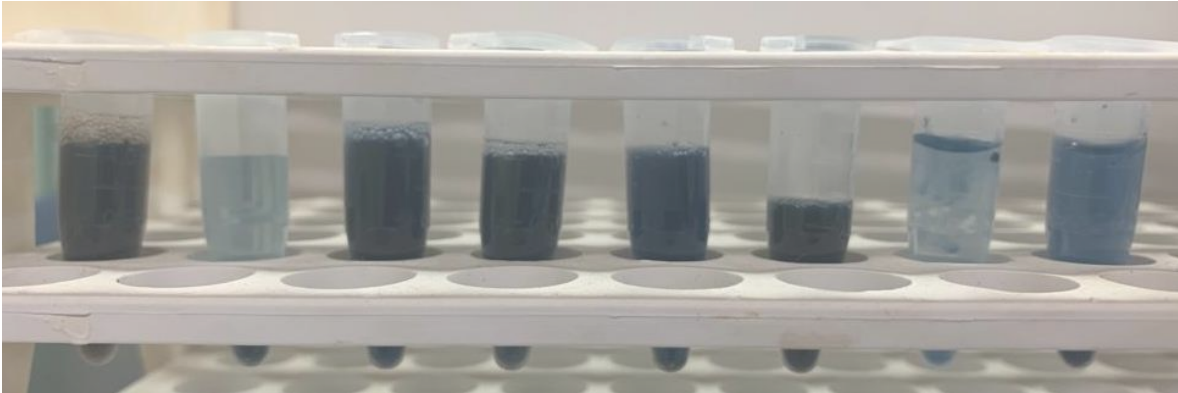


Figure 4.4.1. Solubility test for **System 3** PFCS with acetate, benzoate, bromide, chloride, iodide, MeSO₄, tosylate and salicylate.



4.5. Radical Scavenging Activity

The DPPH free radical scavenging activity of the salts was studied by obtaining the EC₅₀ of **System 1** and **System 3** PFCS with 8 different counterions (*Table 4.4.1.*), and analyzed as a measure equivalent to the antioxidant activity of the salts. All salts showed antioxidant activity in the micromolar range (from 13.27 μM to 271 μM). For **System 1**, the optimal counterion was MeSO₄ and for **System 3**, it was iodide.

Table 4.4.1. EC₅₀ values for the antioxidant activity of **System 1** and **System 3** PFCS with various counterions^{a,b}

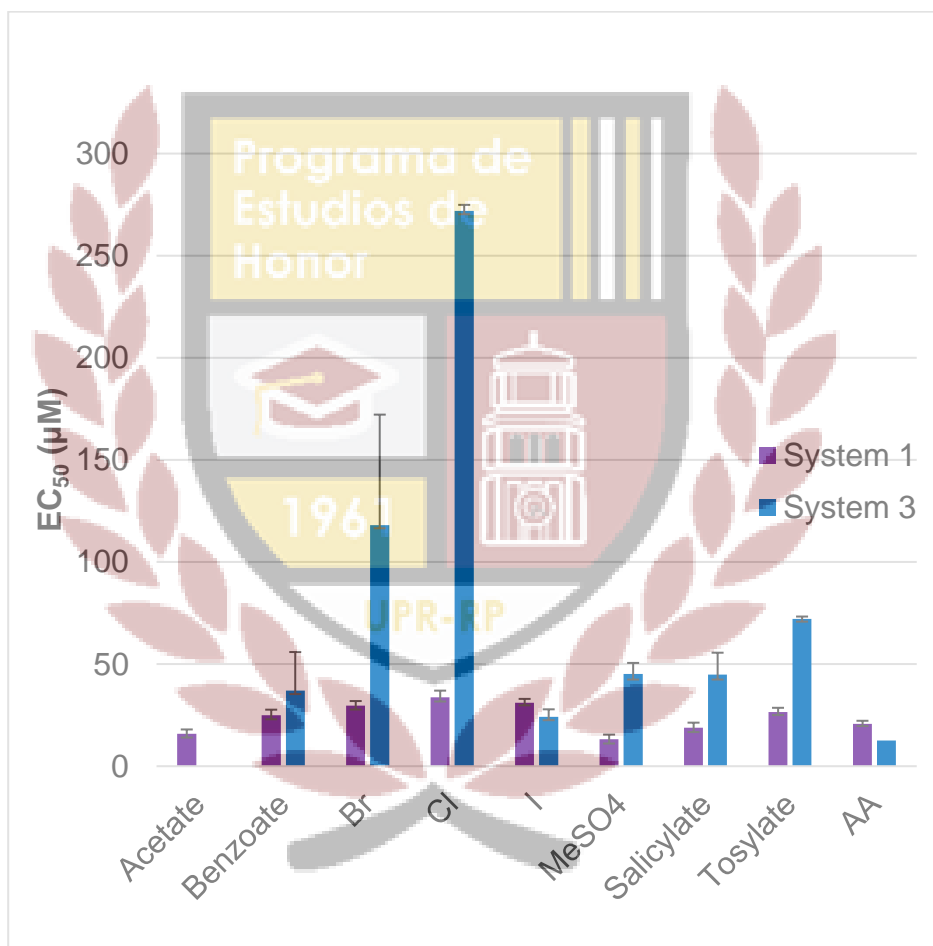
Counterion	System 1	System 3
	EC ₅₀ (μM)	EC ₅₀ (μM)
Acetate	15.91	---
Benzoate	24.96	37.00
Br	29.63	118.00
Cl	33.71	271.90
I	31.00	24.15
MeSO ₄	13.27	45.10
Salicylate	18.90	44.84
Tosylate	26.60	72.05
Ascorbic acid	20.78	12.62

^a EC₅₀ obtained after 15 minutes exposition to DPPH free radical, using ascorbic acid as standard. (n=3)

^b No reliable result was obtained for the EC₅₀ of System 3 acetate PFCS.

When comparing EC₅₀ values obtained for each salt within a PFCS system (Graph 4.4.1), **System 3** salts showed more variable values, as if the antioxidant activity of this system is more dependent on the anion of choice.

Figure 4.4.3. Comparison of radical Scavenging Activity of PFCS from **System 1** and **System 3**, with different counterions



For both systems, aromatic counterions provided an enhanced antioxidant activity, in comparison to halides (except for **System 3** iodide PFCS), which could be attributed to the radical-trapping ability of the aromatic rings due to resonance

stabilization. This high bioactivity might also be related to the low solubility of the salts.

System 1 PFCS showed better antioxidant activity than **System 3** PFCS for each counterion, except for iodide (*Graph 4.4.1*). This trend is typically observed for neutral FC with a variety of heteroaromatic substituents. It is attributed to the electron density on the iron of the ferrocenyl substituent, and its relation to the facility of oxidation of this ion. Lower electron density on Fe^{2+} of **System 1** FC is said to give a higher stability to ferrocene, with a higher tendency to oxidation. However, FC are not only quenchers of free radicals, but can also produce them, acting as prooxidants.³⁷ **System 3** FC has shown to produce these radicals more efficiently due to its lower stability.¹⁷ In different research, the cytotoxic ability of ferrocenyl chalcones has been attributed to their capacity as antioxidants, for example due to their ability to reduce free radicals that damage DNA, or as prooxidants, for example due to their ability to produce free radicals that aid in the disruption of the membranes of microorganisms.³⁷ The results of future bioassays will take this into account.

As mentioned, the electron density surrounding the ferrocenyl moiety affects the antioxidant activity of this group. To study this effect on PFCS, the interaction between cations and anions was analyzed using the Hard and Soft Acids and Bases (HSAB) theory.³⁸ According to this theory, species are classified as hard or soft depending on their size, charge, polarizability, among other properties. Species of the same nature are said to interact more strongly: cations (in this study, $[\text{PFC}^+]$) are considered hard acids and interact strongly with the hard counterparts, anions (in

this study, the counterions).³⁸ This hard-hard compatibility explains their high tendency to form strong ionic bonds. However, the degree of hardness of those charged species depends on their polarizability. This is a measurement of the delocalization of electrons.

Following this analysis, the softest counterions have a high capacity to distribute the electrons of the charged atom across a bigger area. In this manner, the decreasing hardness trend of halides is: Cl (hard) > Br (moderate) > I (soft). The antioxidant activity of **System 3** PFCS paired with halides follows the opposite trend (*Figure 4.4.4.*), with iodide, the softest halide, showing the best antioxidant activity within this category: I > Br > Cl. **System 1** PFCS do not show significantly different EC₅₀ values between halide salts, and do not strictly follow this trend. However, the range of uncertainty could account for this difference, and the activity trend for **System 1** PFCS could be described as: I ≥ Br > Cl. (*Figure 4.4.5.*) Still, bromide showed slightly better antioxidant activity than the iodide salt. A possible explanation to this misalignment of bromide salt in the tendency could be done by considering the unusually upfielded chemical shifts of the ipso carbons on the ¹³C NMR of the bromide salt, discussed earlier (*Table 4.2*). This could be related to an unusually higher electron density on those positions on the [PFC⁺] and, considering that this electron density could affect the overall positive charge, this could explain the higher antioxidant activity that this salt has relative to iodide, without violating the structure-activity tendency that is being analyzed.

In this manner, the softer halides, which have the weakest interaction with the positively charged [PFC⁺], provide the best antioxidant activity. Upon these results,

the positive charge of the pyridinium appears to contribute to the mechanism of action of PFCS.

Figure 4.4.4. Hardness of halides versus **System 3** PFCS antioxidant activity

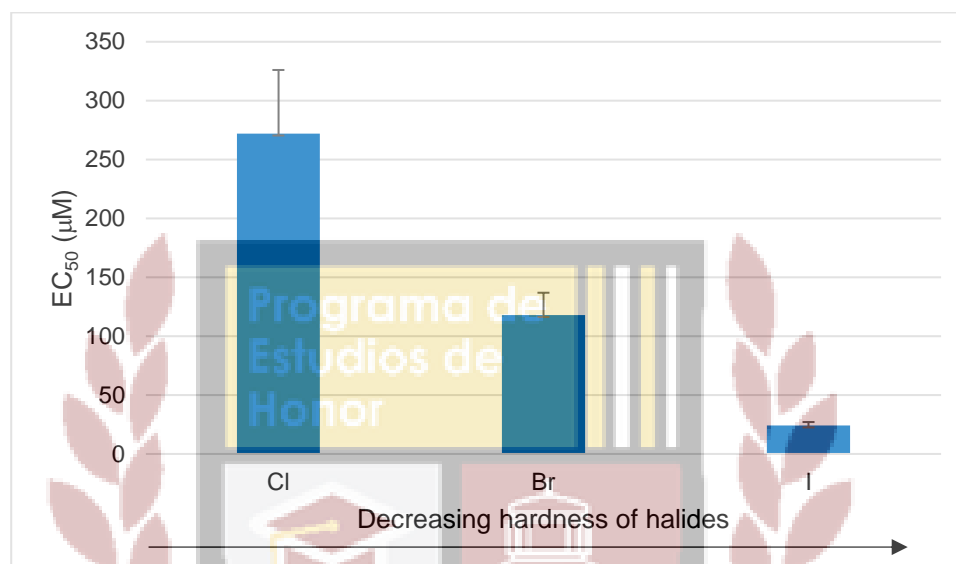
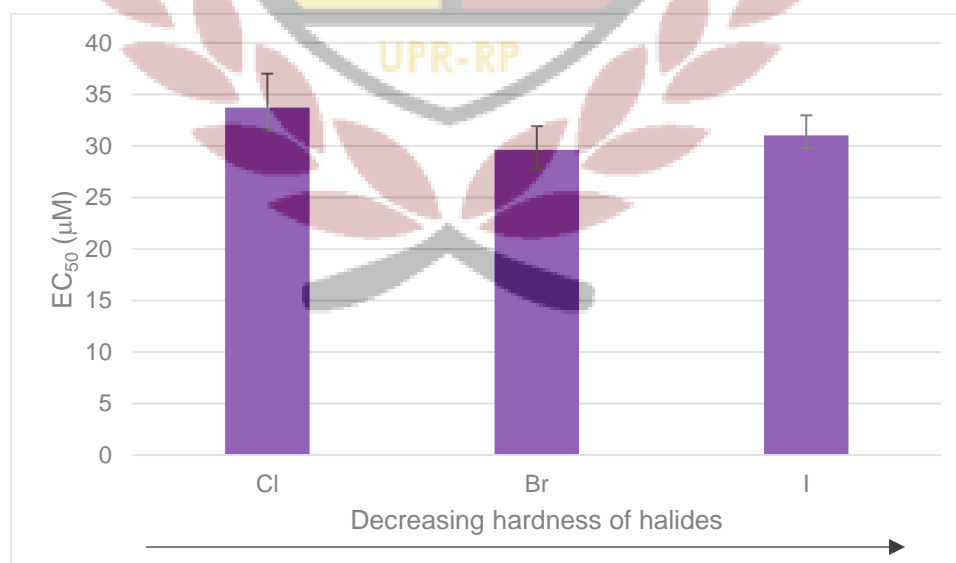


Figure 4.4.5. Hardness of halides versus **System 1** PFCS antioxidant activity



The hardness of the remaining counterions was predicted in terms of their ability to delocalize electrons, considering resonance and induction. The decreasing

hardness trend for the aromatic counterions is expected to be: tosylate > salicylate > benzoate. This trend was further confirmed by modeling the frontier density surfaces for the highest occupied molecular orbital (HOMO) of each counterion (Figure 4.4.6.).

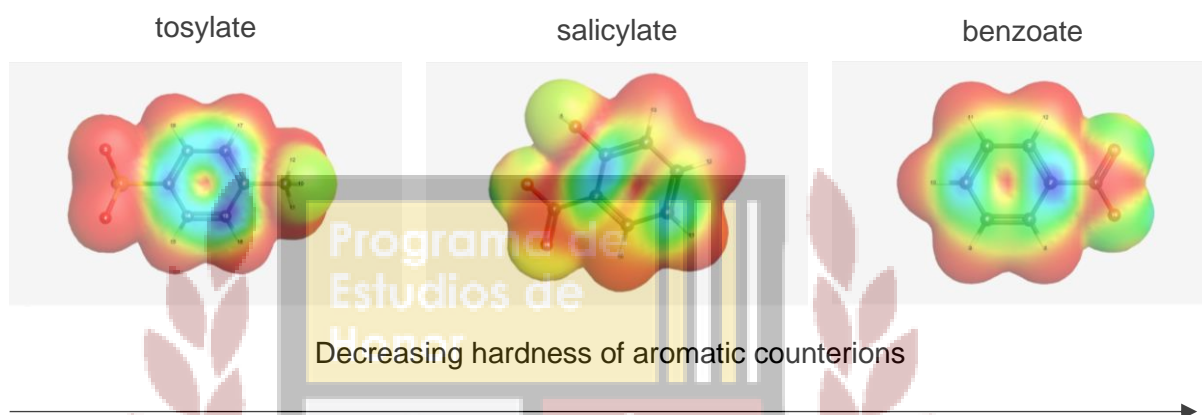
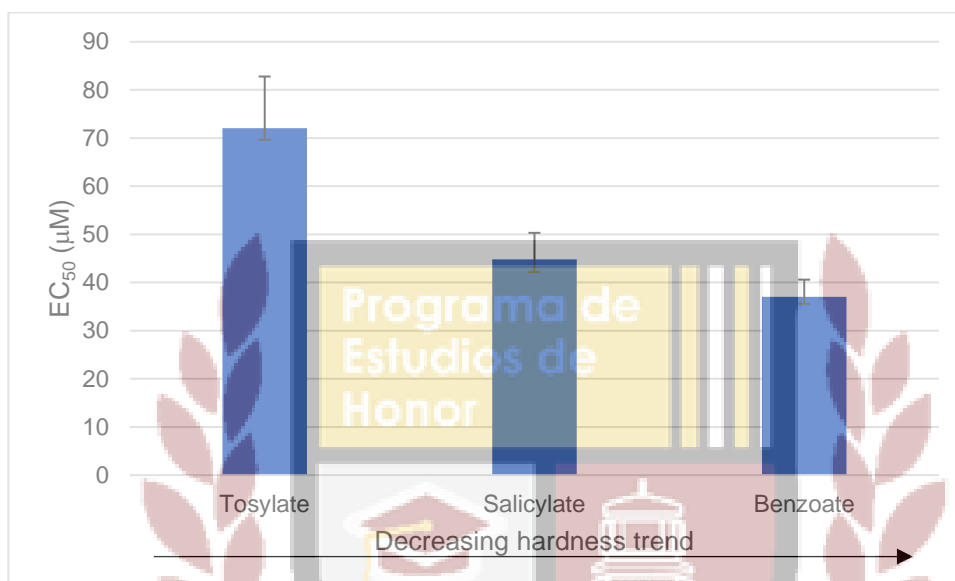


Figure 4.4.6. Frontier density surfaces of aromatic counterions, obtained using WebMO

Although these density maps are commonly used for predicting the probability of a nucleophilic attack, in this discussion they have been used to visualize the electron density of the counterions: blue (higher density) to red (lower density). For the mentioned counterions, the highest electron density can be found on the aromatic rings, as was predicted, due to resonance. However, tosylate shows a higher electron density on this ring, visualized by a bigger blue area in comparison to other counterions. After this sulfonate counterion, the differences between the carboxylate counterions can be explained by considering induction. On salicylate, the hydroxyl substituent donates electron density towards the ring. Again, **System 3** aromatic

PFCS appear to follow a trend: softer counterions provide a better antioxidant activity (*Figure 4.4.7*).

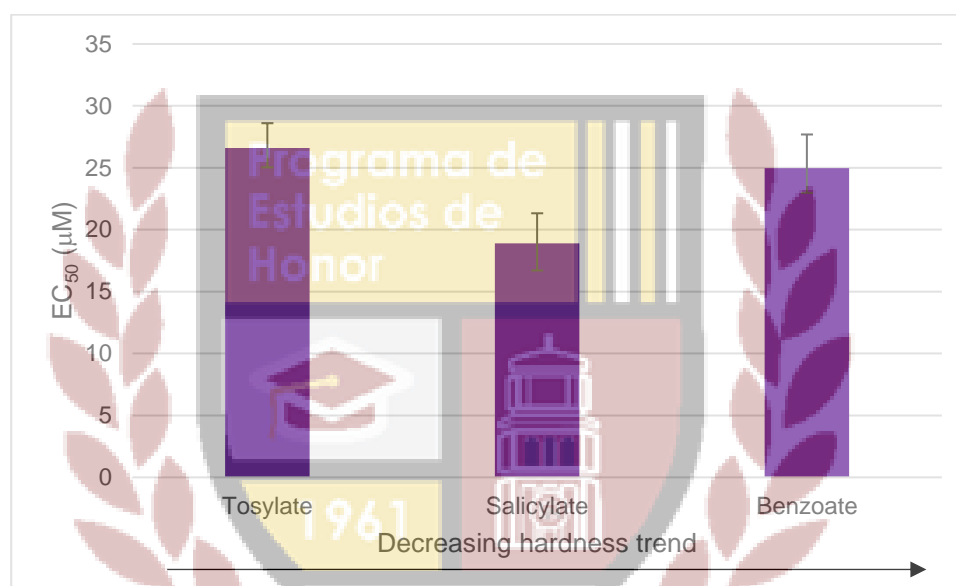
Figure 4.4.7. Hardness of aromatic counterions versus **System 3** antioxidant activity



Apart from the interaction of the anion with the pyridinium cation on [PFC⁺], this trend could be explained by considering the π - π interaction of the aromatic rings with the ferrocenyl moiety, which can be observed on the crystalline structure of **System 3** tosylate (*Figure 4.2.3*). For example, tosylate, having the most dense aromatic ring, could contribute more electron density to ferrocenyl. This could have an overall effect on the [PFC⁺], possibly contributing to the stabilization of the positive charge on the cation. This stabilization of charge is consistent with the mechanism of action that has been proposed for antioxidant ferrocenyl chalcones, as previously mentioned.¹⁷ Again, the degree of positive charge on PFCS appears to be related to the antioxidant activity. However, for **System 1** aromatic PFCS, this trend is not followed, since the decreasing antioxidant activity trend is: salicylate >

benzoate > tosylate (*Figure 4.4.8.*). This could possibly be due to a solubility effect, since it follows the opposite solubility trend (tosylate > benzoate > salicylate). However, one must not conclude that higher solubility leads to less bioactivity, since aromatic rings, overall, provided promising antioxidant activity.

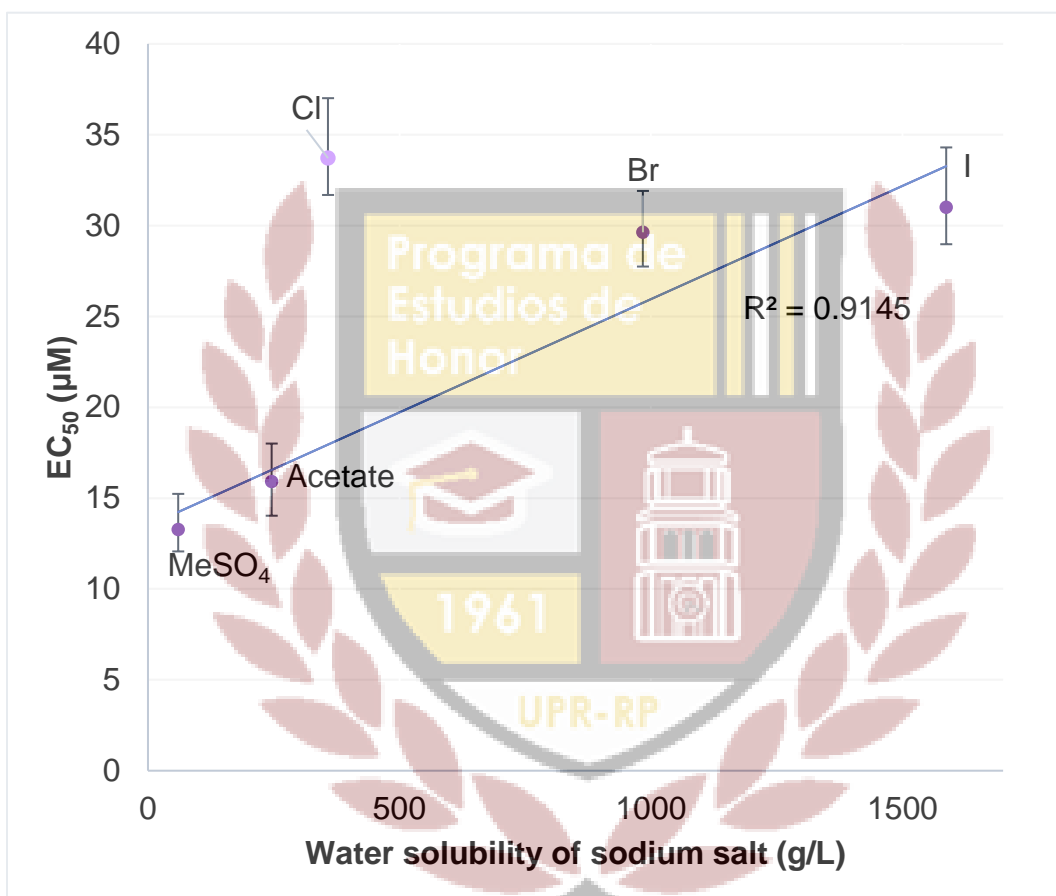
Figure 4.4.8. Hardness of aromatic counterions versus **System 1** antioxidant activity



To further explore the structure-activity relationship for the antioxidant activity of **System 1** PFCS in relation to solubility, values of the solubility of sodium salts were obtained from the literature. The salts considered were only the ones that provided high solubility to **System 1** PFCS. These solubility values were taken as a measure of the solubility of the counterions on their own. This, considering that Na⁺ is present in all salts and, therefore, variations on solubility of the sodium salts should not be attributed to this sodium cation. The solubility of the counterions was found in good inverse correlation ($R^2 = 0.9145$) with the antioxidant activity: the less soluble counterions provided best antioxidant activity (*Figure 4.4.9.*), with the exception of

chloride. However, water solubility for **System 1** PFC salts should be studied by experimentation to confirm this with a much higher reliability.

Figure 4.4.9. Water solubility of sodium salts relationship to the DPPH free radical scavenging activity of **System 1** PFCS



For the analysis of methylated counterions, electron density maps helped visualize that acetate and methylsulfate have a similar hardness (*Figure 4.4.10*). However, acetate shows a more localized electron density than methyl sulfate, which shows orange regions across the anion. This slight delocalization of electrons on methylsulfate might explain why **System 1** PFCS showed a slightly better activity when paired with methylsulfate than acetate (*Table 4.4.1*). However, again, the

EC₅₀ values for these salts do not differ significantly. Future evaluation of the antioxidant activity of **System 3** acetate PFCS will also be subjected to this analysis.

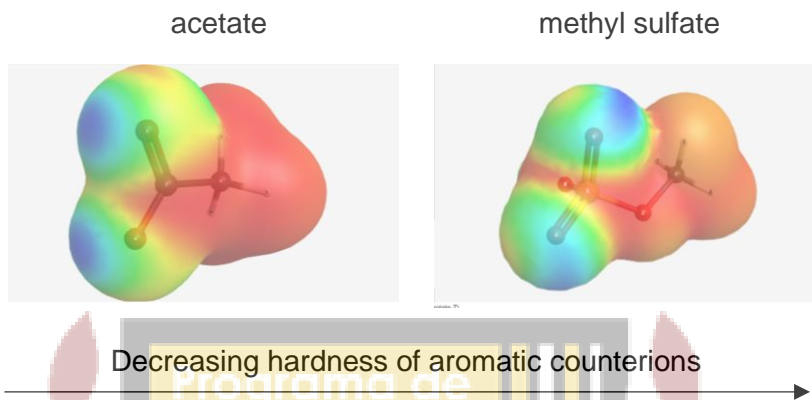


Figure 4.4.10. Frontier density surfaces of methylated counterions, obtained using WebMO.

In future studies, the antioxidant activity of the PFCS will be related to their *in vitro* anticancer and antibacterial activity. The antioxidant tendencies that have been analyzed in relation to the HSAB principle could later provide insight into the mechanism of action of these salts. As preliminary results, the structure-antioxidant activity relationship that has been found is also consistent with the antibacterial activity of **System 3** iodide PFCS, showing a better IC₅₀ than methylsulfate salts. This could possibly be due to the fragile interaction between the hard acid and relatively soft base. This would make the positive charge more available to interact with the negatively charged groups on the membrane of bacteria. In this sense, the counterion could aid on the disruption of the membrane. Future works will elaborate more on these tendencies.

5. CONCLUDING REMARKS

Salts of **System 1** and **System 3** PFCS, with 6 different counterions were prepared by ion exchange chromatography using the halide-to-anion exchange, or vice versa: acetate, benzoate, bromide, chloride, salicylate and tosylate. These salts were studied in addition to the previously reported methylsulfate and iodide salts.¹ NMR, EDS and XRDC characterization confirms the purity of these salts and successful counterion exchanges. All salts appear to have counterion-dependent radical scavenging activity, with EC₅₀ values ranging from 13.27 μM to 271.90 μM in a 15 minute exposition to DPPH. Structure-activity relationships were observed in relation to the system of the PFCS, and properties of the counterions. **System 1** has better activity than **System 3**, possibly due to a difference in electron density on the oxidizable Fe²⁺ ion of ferrocene. **System 3** PFCS appears to be more strongly influenced by the nature of the counterion, with softer counterions providing a better antioxidant activity. The same appears to be true for **System 1** PFCS, but with some exceptions, which could be related to solubility effects. These structure-activity relationships, to some extent, could guide the selection of the optimal counterion of PFCS. Future works include the comparison of the antioxidant activity of the salts with their anticancer and antibacterial activity. These relationships could contribute important information about the mechanism of action of the studied salts, which remains unexplored.

ACKNOWLEDGEMENTS

Dr. Abel Baerga and laboratory

Dr. Dalice Piñero and laboratory


Dr. Liz Díaz and laboratory

Materials Characterization Facilities at UPR Molecular Research Center

The Single Crystal X-Ray Diffraction Instrument was acquired through the support of the National Science Foundation under the Major Research Instrumentation Award Number CHE-1626103.

This project was partially funded by PR-LSAMP under the proposal HRD-1400868.

BIBLIOGRAPHY

- 
- (1) Delgado-Rivera, S. M.; Pérez-Ortiz, G. E.; Molina-Villarino, A.; Morales-Fontán, F.; García-Santos, L. M.; González-Albó, A. M.; Guadalupe, A. R.; Montes-González, I. Synthesis and Characterization of Novel Ferrocenyl Chalcone Ammonium and Pyridinium Salt Derivatives. *Inorg. Chim. Acta* **2017**, *468*, 245–251.
- (2) Delgado-Rivera, S. M. Synthesis and Characterization of Ferrocenyl Chalcone Ammonium and Pyridinium Salt Derivatives. M.S. Thesis. University of Puerto Rico, Río Piedras Campus, 2017.
- (3) Datos de Cáncer. <http://www.rcpr.org/Datos-de-Cáncer/Tasas-y-Mapas> (accessed Nov 18, 2018).
- (4) Siegel, R.; Miller, K.; Jemal, A. Cancer Statistics. *CA Cancer J Clin.* **2019**, *69*, 7-34.
- (5) Malaria. <https://www.who.int/malaria/media/world-malaria-day-2018/en/> (accessed Nov 18, 2018).
- (6) Patra, M.; Gasser, G. The Medicinal Chemistry of Ferrocene and Its Derivatives. *Nat. Rev. Chem.* **2017**, *1* (9), 1-12.

- (7) Dutta, S.; Shome, A.; Kar, T.; Das, P. K. Counterion-Induced Modulation in the Antimicrobial Activity and Biocompatibility of Amphiphilic Hydrogelators: Influence of in-Situ-Synthesized Ag-Nanoparticle on the Bactericidal Property. *Langmuir* **2011**, *27* (8), 5000–5008.
- (8) Paulekuhn, G. S.; Dressman, J. B.; Saal, C. Trends in Active Pharmaceutical Ingredient Salt Selection Based on Analysis of the Orange Book Database Trends in Active Pharmaceutical Ingredient Salt Selection Based on Analysis of the Orange. *J. Med. Chem.* **2007**, 6665–6672.
- (9) Madaan, P.; Tyagi, V. K. Quaternary Pyridinium Salts : A Review. *J Oleo Sci.* **2008**, *215* (4), 197–215.
- (10) Sarapuk, J.; Kleszczyrska, H.; Pernakb, J.; Kalewskab, J.; Rözycka-roszak, B. Influence of Counterions on the Interaction of Pyridinium Salts with Model Membranes. *Z Naturforsch C.* [Online] **1999**, 2–5. <https://www.ncbi.nlm.nih.gov/pubmed/10627994> (accessed November, 2018).
- (11) McCarthy, J. S.; Rückle, T.; Djeriou, E.; Cantalloube, C.; Ter-Minassian, D.; Baker, M.; O'Rourke, P.; Griffin, P.; Marquart, L.; Hooft Van Huijsduijnen, R.; et al. A Phase II Pilot Trial to Evaluate Safety and Efficacy of Ferroquine against Early Plasmodium Falciparum in an Induced Blood-Stage Malaria Infection Study. *Malar. J.* **2016**, *15* (1), 1–9.
- (12) Wiedmann, T. S.; Naqwi, A. Pharmaceutical Salts: Theory, Use in Solid Dosage Forms and in Situ Preparation in an Aerosol. *Asian J. Pharm. Sci.* **2016**, *11* (6), 722–734.

- (13) Nielsen, S. F.; Larsen, M.; Boesen, T.; Schønning, K.; Kromann, H. Cationic Chalcone Antibiotics. Design, Synthesis, and Mechanism of Action. *J. Med. Chem.* **2005**, *48* (7), 2667–2677.
- (14) Kumar, L.; Meena, C. L.; Pawar, Y. B.; Wahlang, B.; Tikoo, K.; Jain, R.; Bansal, A. K. Effect of Counterions on Physicochemical Properties of Prazosin Salts. *AAPS PharmSciTech* **2013**, *14* (1), 141–150.
- (15) David, S. E.; Timmins, P.; Conway, B. R. Impact of the Counterion on the Solubility and Physicochemical Properties of Salts of Carboxylic Acid Drugs. *Drug Dev. Ind. Pharm.* **2012**, *38* (1), 93–103.
- (16) Zhang, C.; Jiang, Y.; Ju, H.; Wang, Y.; Geng, T. “Organic counterion” modified quaternary ammonium salt: Impact on antibacterial activity & application properties. *J Mol Liq.* **2017**, *241*, 638-645.
- (17) Wu, X.; Tiekink, E. R. T.; Kostetski, I.; Kocherginsky, N.; Tan, A. L. C.; Khoo, S.; Wilairat, P.; Go. M. Antiplasmodial Activity of Ferrocenyl Chalcones: Investigations into the Role of Ferrocene. *Eur J Pharm Sci.* **2006**, *27*, 175-187.
- (18) Mannava, M. K. C.; Suresh, K.; Nangia, A. Enhanced Bioavailability in the Oxalate Salt of the Anti-Tuberculosis Drug Ethionamide. *Cryst. Growth Des.* **2016**, *16* (3), 1591–1598.
- (19) Bastin, R. J.; Bowker, M. J.; Slater, B. J. Salt Selection and Optimisation Procedures for Pharmaceutical New Chemical Entities. *Org. Process Res. Dev.* **2000**, *4* (5), 427–435.
- (20) Kumar, L.; Amin, A.; Bansal, A. K. Preparation and Characterization of Salt Forms of Enalapril. *Pharm. Dev. Technol.* **2008**, *13* (5), 345–357.

- (21) Christiansen, S. H.; Murphy, R. A.; Juul-Madsen, K.; Fredborg, M.; Hvam, M. L.; Axelgaard, E.; Skovdal, S. M.; Meyer, R. L.; Sørensen, U. B. S.; Möller, A.; et al. The Immunomodulatory Drug Glatiramer Acetate Is Also an Effective Antimicrobial Agent That Kills Gram-Negative Bacteria. *Sci. Rep.* **2017**, 7 (1), 1–16.
- (22) Gao, Z. Evaluation of Different Kinds of Organic Acids and Their Antibacterial Activity in Japanese Apricot Fruits. *African J. Agric. Reseach* **2012**, 7 (35), 4911–4918.
- (23) Patnala, S. R. C. M.; Khagga, M.; Bhavani, R.; Bhavani, V. Novel Salt of Tinidazole with Improved Solubility and Antibacterial Activity. *Orient. J. Chem.* **2017**, 33 (1), 490–499.
- (24) Healthcare, G. Ion Exchange Chromatography & Chromatofocusing: Principles and Methods. *GE Heal. Handbooks* **2016**, 170.
- (25) Introduction, A.; Methods, I. An Introduction to Ion-Exchange Methods. *J. Chromatogr. Libr.* **1990**, 46 (C), 15–27.
- (26) Pohl, C. A. Novel Method for Manipulation of Anion-Exchange Selectivity by Derivatizing Hydroxyl Groups in the Proximity of Quaternary Nitrogen Ion-Exchange Sites with Glycidol. *Talanta* **2018**, 177 (September 2017), 18–25.
- (27) Alcalde, E.; Dinarès, I.; Ibáñez, A.; Mesquida, N. A Simple Halide-to-Anion Exchange Method for Heteroaromatic Salts and Ionic Liquids. *Molecules* **2012**, 17 (4), 4007–4027.
- (28) Yan, H. C.; Li, Q. X.; Geng, T.; Jiang, Y. J. Properties of the Quaternary Ammonium Salts with Novel Counterions. *J. Surfactants Deterg.* **2012**, 15 (5), 593–599.

- (29) Passeri, R.; Aloisi, G. G.; Elisei, F.; Latterini, L.; Caronna, T.; Fontana, F.; Sora, I. N. Photophysical Properties of N-Alkylated Azahelicene Derivatives as DNA Intercalators: Counterion Effects. *Photochem. Photobiol. Sci.* **2009**, *8* (11), 1574.
- (30) Ko, G.; Schaefer, T.; Bock, E. π -Electron densities in the pyridinium cation: the effect of the counterion on the proton magnetic resonance spectrum. *Can J Chem.* **1964**, *42*, 2541-2548.
- (31) Liu, Z.; Hao, F.; Xu, H.; Wang, H.; Wu, J.; Tian, Y. A- π -D- π -A Pyridinium Salts: Synthesis, Crystal Structures, Two-Photon Absorption Properties and Application to Biological Imaging. *CrystEngComm*. [Online] **2015**. (accessed November, 2018)
- (32) Sanabria-Ríos et al. Antibacterial activity of 2-alkynoic fatty acids against multidrug-resistant bacteria. *Chem. Phys. Lipids.* **2014**, *178*, 84–91.
- (33) Vašková, J. et Al. Some ferrocenyl chalcones as useful candidates for cancer treatment. *In Vitro Cellular & Developmental Biology – Animal.* **2015**, *51*, 964-974.
- (34) Sharma, O.; Bhat, T. DPPH antioxidant assay revisited. *Food Chemistry.* **2009**, *113*, 1202-1205.
- (35) Attar, S. et Al. Ferrocenyl chalcones versus organic chalcones: A comparative study of their nematocidal activity. *Bioorg Med Chem.* **2011**, *19*, 2055-2073.
- (36) Nabi, G.; Liu, Z. [Online] Ferrocenyl chalcones: Antioxidants or prooxidants in dacial-induces oxidation of DNA? *Med Chem Res.* **2011**, *21*. 10.1007/s00044-011-9836-5
- (37) Xiang, W. Investigation on the antiplasmodial activity of ferrocenyl chalcones. B.Sc., Peking University, Singapore, 2005.

(38) Reed, J. Hard and soft acids and bases: Atoms and Atomic Ions. *Inorg. Chem.*
2008, *47*, 5591-5600.



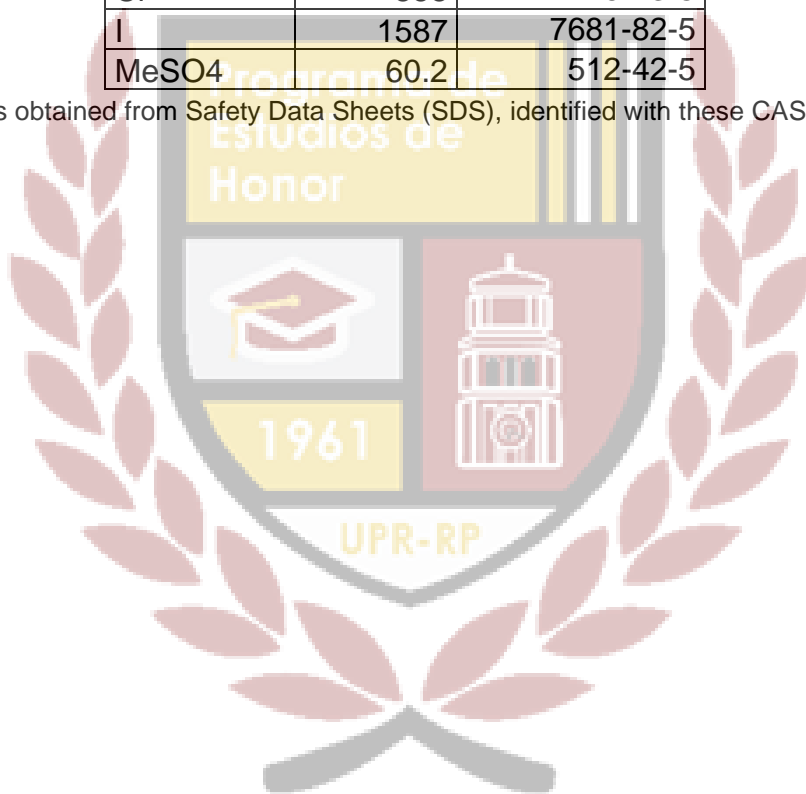
Appendix A

Data obtained from the literature

Table 1. Solubility of sodium salts with various counterions at 20 °C ^a

Counterion	Solubility (g/mL)	CAS
Acetate	246	127-09-3
Br	984	7647-15-6
Cl	358	7440-23-5
I	1587	7681-82-5
MeSO ₄	60.2	512-42-5

^aData was obtained from Safety Data Sheets (SDS), identified with these CAS numbers.





12 de diciembre de 2019

Estudiantes egresados del PREH Segundo Semestre 2018-2019

Eunice Pérez Medina, Ed.D.
Directora

SOLICITUD DE AUTORIZACIÓN PARA PUBLICACIÓN DE TESINA/PROYECTO CREATIVO EN REPOSITORIO DIGITAL DEL SISTEMA DE BIBLIOTECAS DE LA UPR Y PÁGINA WEB DEL PREH

Las tesinas y proyectos creativos de los estudiantes del Programa de Estudios de Honor (PREH) del Recinto de Río Piedras son producciones académicas de muy alta calidad. Por esta razón, el PREH como política las hace disponibles a la comunidad académica y al público en general a través de Sistema de Bibliotecas de la Universidad de Puerto Rico y la página web del PREH en <http://preh.uprrp.edu/>

Con el fin de proteger sus derechos de autor, es necesaria una autorización escrita del autor. Deberá completar y firmar el formulario que se incluye a continuación. Envíe el mismo a programa.honor@upr.edu.

Se incluye la copia digital de su tesis/proyecto creativo. Agradecería que revise la misma antes de firmar y devolver el formulario de autorización en la parte inferior.

AUTORIZACIÓN PUBLICACIÓN DIGITAL DE TESINA/PROYECTO CREATIVO

<input checked="" type="checkbox"/> sí <input type="checkbox"/> no	es la versión final de mi tesis/proyecto creativo. De no ser la versión final, favor de remitir al PREH la versión correcta junto con este formulario.
<input checked="" type="checkbox"/> sí <input type="checkbox"/> no	autorizo la publicación de mi tesis/proyecto creativo en el repositorio digital del Sistema de Bibliotecas del Recinto de Río Piedras.
<input checked="" type="checkbox"/> sí <input type="checkbox"/> no	autorizo la publicación de mi tesis/proyecto creativo en la página web del PREH.

Daisy Díaz Rohena

Nombre completo del autor
(letra de molde)

Daisy Díaz Rohena

Firma

26/ enero/2020

Fecha

Ingrid Montes